Enhanced Oil Recovery (EOR) Using Dielectric Nanoparticles Subjected In Electromagnetic (EM) Wave

By

ZUMIRA NURSHUHADA BINTI ABDULLAH

DISSERTATION REPORT

Submitted to the Electrical & Electronics Engineering Programme
in Partial Fulfillment of the Requirements
for the Degree
Bachelor of Engineering (Hons)
(Electrical & Electronics Engineering)

Universiti Teknologi PETRONAS
Bandar Seri Iskandar
31750 Tronoh
Perak Darul Ridzuan

© Copyright 2011
by
Zumira Nurshuhada binti Abdullah, 2011

CERTIFICATION OF APPROVAL

Enhanced Oil Recovery (EOR) Using Dielectric Nanoparticles Subjected In Electromagnetic (EM) Wave

by

Zumira Nurshuhada binti Abdullah

A dissertation report submitted to the
Electrical & Electronics Engineering Programme
Universiti Teknologi PETRONAS
in partial fulfilment of the requirement for the
Bachelor of Engineering (Hons)
(Electrical & Electronics Engineering)

Approved:

Professor Dr. Noorhana Yahya
Dean, Faculty of Science & Information Technology

Prof. Dr. Noorhana Yahya
Project Supervisor

UNIVERSITI TEKNOLOGI PETRONAS
TRONOH, PERAK

May 2011

CERTIFICATION OF ORIGINALITY

This is to certify that I am responsible for the work submitted in this project, that the original work is my own except as specified in the references and acknowledgements, and that the original work contained herein have not been undertaken or done by unspecified sources or persons.

Zumira Nurshuhada binti Abdullah

ABSTRACT

High viscosity of oil related to high interfacial tension between oil and brine water. To reduce this high interfacial tension, we proposed new method by using nanofluid injection with the aid of electromagnetic (EM) wave. Dielectric nanofluids will polarize at low frequency of 1 kHz. Dielectric nanoparticles of ZnO,CoO and Al_2O_3 were synthesized by using sol gel method and was characterize using X-Ray Diffractometer (XRD), Field Emission Scanning Electron Microscope (FESEM), Energy Dispersive X-Ray (EDX) and RAMAN Spectroscopy.ZnO has lower atomic deviation of 3.08%, small crytallite size of 12.27 nm,and have high dielectric constant of 3xE6.Nanopowder were mixed with stabilizer, Sodium Dodecyl Sulphate (SDS) before injected into the column.The nanofluid mixed with 1% SDS stay suspended for a month duration. 22 cm lenght of Polyvinyl Chloride (PVC) column filled with 535.81 mD glass beads was flooded with 20 kppm of brine water and with crude oil viscosity of 16.31 cp.Water flooding performed before continue with nanofluids injection. From oil recovery experiment, ZnO yields the highest recovery factor which is 31 % compared to CoO and Al_2O_3 which only have recovery factor of 12.5% and 10 % respectively.This is a new contribution towards the industry as the role of EM wave to activate the ZnO is significant.

ACKNOWLEDGEMENTS

In the name of Allah, The Most Merciful and Compassionate

Heartiest gratitude to Professor Dr Noorhana binti Yahya,the supervisor of this project,for her invaluable guidance and encouragement extended throughout the study.Her continuous supervision,suggestion,patience and guidance deserve a special mention.

A special thank also goes to Miss Noor Rasyada, Miss Poppy Puspitasari for their co-operation in helping me to prepare samples and their assistance along way to complete this thesis.

In addition, I would like to thanks my colleagues for their constructive comments and knowledge sharing during the progress of this thesis. I also would like to acknowledge staffs from Electrical & Electronics Engineering, Geosciences and Petroleum Engineering, Chemical Engineering, Mechanical Engineering and Civil Engineering for giving me permission to do necessary research works and use the facilities under their supervision.

To my beloved parents, I would like to express sincere gratitude for their continuous support and encouragement towards the success of this project

TABLE OF CONTENTS

LIST OF TABLES ix

LIST OF FIGURES ..... x-xii

CHAPTER 1 INTRODUCTION 1

1.1 Background of Study 1

1.2 Problem Statement 3

1.3 Objective and Scope of Study 4

CHAPTER 2 LITERATURE REVIEW AND THEORY 5

2.1 Enhanced Oil Recovery (EOR) 5

2.2 Dielectric Nanoparticles 6

2.3 Sol Gel Technique for Preparation of Metal Oxide 7

2.4 Interfacial Tension 8

2.5 Polarization Mechanisms 10

CHAPTER 3 METHODOLOGY 13

3.1 Procedure Identification 13

3.2 Tools and Equipment Required 14

3.2.1 Characterization Equipment 14

3.2.2 Hardware 18

CHAPTER 4 RESULT AND DISCUSSION 22

4.1 Synthesis of Metal Oxide 22

4.1.1 Experimental Procedure 22

4.1.2 Calculation of Metal Oxide Using Sol Gel Method 22

4.1.3 Sol Gel Method Procedure 25

4.2 Characterization of Nanopowder 27

4.2.1 X-Ray Diffraction (XRD) Results 27

4.2.2 Field Emission Scanning Electron Microscope (FESEM) Result 33

4.2.3 Energy Dispersive X-Ray (EDX)Result 36

4.2.4 RAMAN Spectroscopy Result 41

4.3 Petrophysical Characterization 45
4.3.1 Beads Mixture 45
4.3.2 Permeability Test 46
4.3.3 Porosity Test 48
4.3.4 Stability Test 49
4.3.5 Dielectric Characterization 51
4.4 Oil Recovery Experiment 55

CHAPTER 5 CONCLUSION AND RECOMMENDATION 65
5.1 Conclusion 65
5.1 Recommendation 66

LIST OF TABLES

Table 1 Factor influencing recovery of petroleum 5

Table 2 Calculations for metal oxide 24

Table 3 Annealing temperature and duration for each sample 26

Table 4 Standard Card of Zinc Oxide, CoO and Al_2O_3 27

Table 5 XRD data of metal oxide samples with different annealing temperatures 31

Table 6 Atomic Percentage of Element 38

Table 7 EDX data and standard deviation for ZnO at 350°C and 450°C 39

Table 8 EDX data and standard deviation for CoO at 300°C and 400°C 39

Table 9 EDX data and standard deviation for Al_2O_3 at 1000°C and 1100°C 39

Table 10 Nanopowder intensity with respect to its RAMAN shift 43

Table 11 Glass Beads Combination 45

Table 12 Measurement of Permeability Test 47

Table 13 Measurement of Porosity Test 48

LIST OF FIGURES

Figure 1 CO_2 injection for EOR 2

Figure 2 Solvent injection for EOR 2

Figure 3 Steam injection EOR 2

Figure 4 Porosity 3

Figure 5 Illustration how surface area increases as the size is reduced 5

Figure 6 Electric and magnetic field propagation 7

Figure 7 Illustration of Internal Tension of Different Liquids 8

Figure 8 The current in a capacitor containing a lossy dielectric 10

Figure 9 Schematic representation of the different polarization mechanisms 11

Figure 10 Contribution of the different polarization mechanisms to the frequency dependence of the relative permittivity 12

Figure 11 Flowchart of project 13

Figure 12 The Diffractometer 15

Figure 13 FESEM Equipment 16

Figure 14 LCR vector network analyzer 17

Figure 15 Data Acquisition System 18

Figure 16 Fluxgate Magnetometer 18

Figure 17 Function Generator 18

Figure 18 DC Power Supply 19

Figure 19 Balance Machine 19

Figure 20 Pressure Gauge 20

Figure 21 Viscometer 20

Figure 22 Variety size of spindle 20

Figure 23 Consol Drive Pump 21

Figure 24 PVC Column 21

Figure 25 Raw material used 22

Figure 26 Stirring process 25

Figure 27 Gel formed 25

Figure 28 After drying process 25

Figure 29 Crushing process 25

Figure 30 Annealing equipment 26
Figure 31 XRD result for ZnO 350°C sample 28
Figure 32 XRD result for ZnO450°C sample 28
Figure 33 Comparison XRD result for ZnO 350°C and 450°C sample..... 28
Figure 34 XRD result for CoO 300°C sample 29
Figure 35 XRD result for CoO 400°C sample 29
Figure 36 Comparison XRD result for CoO 300°C and 400°C sample 29
Figure 37 XRD result for Al_2O_3 at 1000°C sample 30
Figure 38 XRD result for Al_2O_3 at 1100°C sample 30
Figure 39 Comparison XRD result for Al_2O_3 1000°C and 1100°C sample 30
Figure 40 FESEM morphology for ZnO at 350°C 33
Figure 41 FESEM morphology for ZnO at 450°C 33
Figure 42 FESEM morphology for CoO at 300°C 34
Figure 43 FESEM morphology for CoO at 400°C 34
Figure 44 FESEM morphology for Al_2O_3 at 1000°C 35
Figure 45 FESEM morphology for Al_2O_3 at 1100°C 35
Figure 46 Spectrum and EDX data for ZnO 350°C 36
Figure 47 Spectrum and EDX data for ZnO450°C 36
Figure 48 Spectrum and EDX data for CoO 300°C 37
Figure 49 Spectrum and EDX data for CoO 400°C 37
Figure 50 Spectrum and EDX data for Al_2O_3 1000°C 37
Figure 51 Spectrum and EDX data for Al_2O_3 1100°C 38
Figure 52 Spectrum RAMAN data for ZnO 350°C sample 41
Figure 53 Spectrum RAMAN data for ZnO 450°C sample 41
Figure 54 Spectrum RAMAN data for Cobalt Oxide 300°C sample 42
Figure 55 Spectrum RAMAN data for Cobalt Oxide 400°C sample 42
Figure 56 Spectrum RAMAN data for Al_2O_3 1000°C sample 42
Figure 57 Spectrum RAMAN data for Al_2O_3 1100°C sample 43
Figure 58 Glass Beads Mixture..... 45
Figure 59 Experiment Set Up for Permeability Test 47
Figure 60 Three concentrations of ZnO nanofluids 49
Figure 61 Three concentrations of CoO nanofluids 50

Figure 62 Three concentrations of Al_2O_3 nanofluids 50
Figure 63 16452A Test Fixture 51
Figure 64 Dielectric characterization for ZnO nanofluid 52
Figure 65 Dielectric characterization for CoO nanofluid 53
Figure 66 Dielectric characterization for Al_2O_3 nanofluid 53
Figure 67 Experiment Set Up for Oil Recovery Experiment 55
Figure 68 Oil recovered by using ZnO nanaofluid 58
Figure 69 Oil recovered by using CoO nanaofluid 61
Figure 70 Oil recovered by using Al_2O_3 nanaofluid 64

LIST OF ABBREVIATIONS

r.p.m	rotation per minute
CO_2	Carbon Dioxide
EOR	Enhanced Oil Recovery
N_2	Nitrogen
OOIP	Original Oil In Place
PVC	Polyvyniyl Chloride
ROIP	Residual Oil In Place
SDS	Sodium Dodecyl Sulphate

CHAPTER 1

INTRODUCTION

1.1 Background of Study

Oil will continue to account for the largest share in the world's primary energy mix up to 2030 at least. Demand is expected to grow by 57% from 2002 to 2030. The IEA World Economic Outlook for 2004 projects in its Reference Scenario : an unabated growth of oil supply from 77 million barrels per day (mb/d) in 2000 to 121.3 mb/d in 2030 (IEA 2004).

According to the World Energy Outlook 2004 there are sufficient oil resources in place for the period up to 2030, provided that sufficient investments are made and that new technologies for improved oil recovery (IOR) or enhanced oil recovery (EOR) are available (IEA 2004) [1].

Oil production can be categorized into three phases: primary, secondary and tertiary, which is EOR. Primary oil recovery is limited to hydrocarbons that naturally rise to the surface, or those that use artificial lift devices, such as pump jacks. Secondary recovery employs water and gas injection, displacing the oil and driving it to the surface. EOR includes thermal, chemical and miscible gas processes which is injecting substances into the reservoir that are not naturally found there [2].

The past and ongoing research into EOR can be roughly divided into 3 general areas :

1. Gas injection, including CO_2, N_2, flue.
2. Chemical,including surfactant, surfactant with polymer, surfactant with foam.
3. Thermal,including convention steam, steam assisted gravity drainage, cyclic injection, and in-situ combustion.

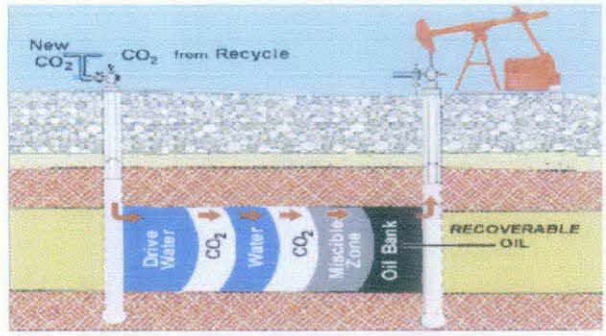

Figure 1 : CO_2 injection for EOR

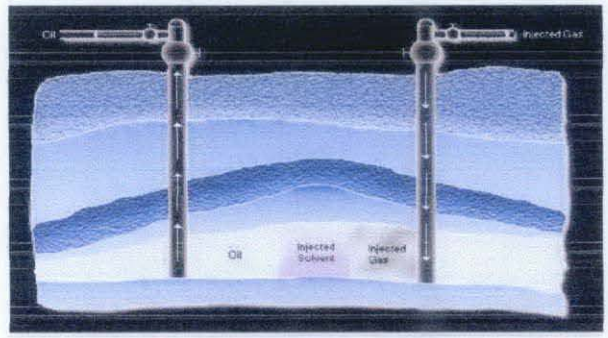

Figure 2: Solvent injection for EOR

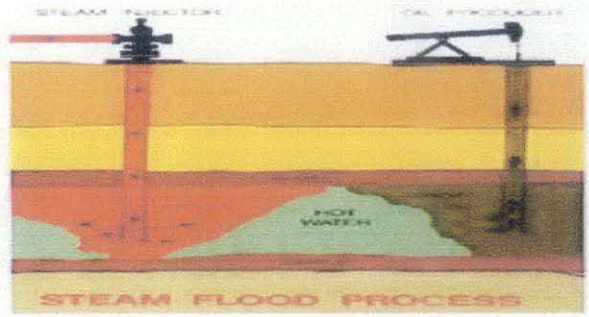

Figure 3 : Steam injection for EOR

1.2 Problem Statement

Almost all oil and gas is found within the tiny spaces in sedimentary rocks, mainly sandstone and coarse-grained limestones. A piece of sandstone or limestone is very much like a hard sponge, full of holes, but not compressible. These holes, or pores, can contain water, oil or gas, and the rock will be saturated with water, oil or gas. The holes are much tinier than sponge holes, but they are still holes, and they are called porosity.

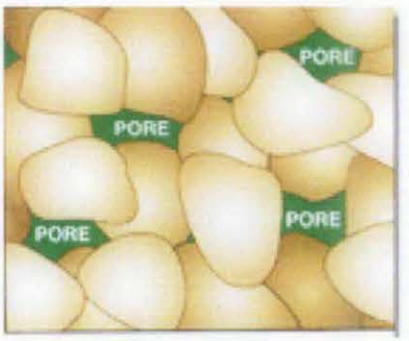

Figure 4 : Porosity

The oil and gas become trapped in these holes, for millions of years, until someone come to find it and get it out. The oil is trapped inside the rock's porosity. High pressure below 1000 meter cause high viscosity of oil and this remains a challenge for industry. Thus, to overcome this challenge, we propose a new method to recover the remaining oil by using nanoparticles subjected in EM wave.

1.3 Objective and Scope of Study

1.3.1 Objectives

The purpose of this project is to find best dielectric nanoparticles in order to improve oil recovery by reducing the interfacial tension between oil and core rock.

The objectives of this project are:

- To synthesis dielectric nanoparticles by using sol-gel method.
- To characterize the dielectric nanoparticles by using X-Ray Diffractions (XRD), Field Emission Scanning Electron Microscope (FESEM), Energy Dispersion X-ray Spectroscopy (EDX), RAMAN Spectroscopy and also dielectric properties.
- To test the ability of dielectric nanoparticle to improve the oil recovery using EM transmitter.

1.3.2 Scope of study

The area of study for this project will be divided to 2 parts: first part is synthesis and characterize the nanoparticle detector. Second part is the experiment of oil recovery which consists of transmitter, fluxgate magnetometer, core rock sample as well as the environment to be applied. The scope of study covers for:

- The material and method to develop the dielectric nanoparticles material
- To carry out some petro physical experimental works.
- To calculate the oil recovery for core sample.

CHAPTER 2

LITERATURE REVIEW

2.1 Enhanced Oil Recovery (EOR)

As we already know, oil recovery is remained a challenge because of the environment under the sea floor. In 1927, Uren and Fahmy investigated a number of factors which affect the recovery of petroleum from unconsolidated sands [3].Table 1 show the lists of the factor that affect the petroleum exploration.

Table 1 : Factors influencing recovery of petroleum

Factor (Condition)	Condition for maximum recovery	Actual Value of "Variable" giving best recovery	Maximum recovery of oil at "Best Condition" % O.I.P.
1. Grain size	Largest grain size	20 to 40 mesh	41.3
2. Porosity	Highest porosity	41.1%	37.5
3. Variable grain size or texture	Most uniform	(all 40-48 mesh)	54.8
4. Coating on grains (wettability)	Smooth Carbon	Intermediate wettability	84
5. Oil viscosity	Lower oil viscosity	≈ 1 cp (gasoline)	67
6. Temperature	Highest temp.	125°F	70.5
7. Rate	Slow rates (with additives)	< 1 ft/day	59.0
8. Interfacial tension	Lowest IFT	8 dynes/cm	71
9. Salts in solution (acid or alkaline)	Highly alkaline	1.0 Normal sodium carbonate solution (also lowest IFT).	71

Thus, in order to improve oil recovery,the interfacial tension between oil and brine water need to be reduce first. By reducing the interfacial tension to 8 dynes/cm,it will produce maximum recovery of 71 % at best condition.

Zhang Jihong, Yu Haiming had done study on EOR by DC electric field in water flooding reservoir. They found that seepage flow behavior under the positive applied DC electric field, electrodynamic and electrohydraulic seepage flow velocity increase with the electric field strength. The results of the oil displacement experiments indicate that the core samples reveal strongly water-wet property, irreducible water saturation increase and residual oil saturation decrease, and oil recovery of water drive improved more than 5% [4].

2.2 Dielectric Nanoparticles

Nanoparticles are particles ranging from 1 nanometer to 100 nanometer.One of the important characteristics of nanoparticles is their large ratio of surface area to volume (compared to bulk materials).When the size decrease, new visible or usable areas are added while the total volume remains the same.Below illustrate the increase in surface area with respect to reducing the size of particles.

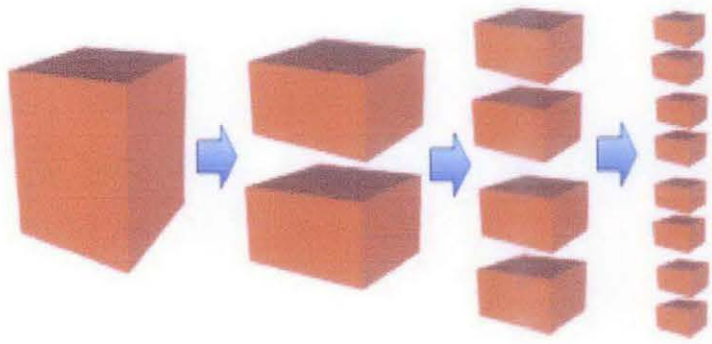

Figure 5 : Illustration how surface area increases as the size is reduced

Large surface area makes some nanoparticles highly soluble in liquids.A 30 nanometer iron particle has 5% of its atoms on the surface while the remaining reside inside. However, a 3 nm particle has 50% of its atoms on the surface. The atoms on the surface, which are not bonded on one side, are far more active than the atoms residing inside (which are bonded all around, thus they are "satisfied"). An increase in surface area therefore leads to an increase in reactivity [5].

Synthsizing metal oxide can be performe by using solgel method.According to C.X.XU,zinc oxide annealed at 600◦C,650◦C,700◦C ,show hexagonal structure [6].For cobalt oxide , increasing the decomposition temperature, the Bragg peaks become sharper and the intensity rises, respectively [7]. Powders are homogeneously dispersed and sometime cluster arranged (dimensions ranging from 300 to 400 nm) [8].Metal oxide aluminium oxide can be synthesized to get The SEM images confirm that individual particles are effectively spherical and that there is a large size range from ~100 to 2000nm [9].

2.3 Sol Gel Technique for Preparation of Metal Oxide

The sol-gel process is a wet-chemical technique widely used recently in the fields of materials science and ceramic engineering.Using this method the size of particles can be controlled by starting conditions. Among various synthesis methods for metal oxides, sol gel process offers several advantages ocer other methods including good homogeity,simple ,and high purity [10].

The sol-gel method is a useful and attractive technique for the preparation of nanosized particles because of its advantages which is good stoichiometric and the production of ultrafine particles with a narrow size distribution in a relatively short processing time at lower temperatures [11].

According to Daniel Niznansky project, crystalisation of iron oxide occures during the heating above 800°C. This metastable state can be achieved by sol-gel process [12].

He again proved that by using sol gel method,SiO2 powders doped with magnetic nanoparticles yields small nanoparticles of iron crystals size of 5 nm [13].

2.4 Interfacial Tension

The interfacial tension of liquid is an important physical property that is useful in determining the behavior of liquids in such emulsions, and enhanced oil recovery processes.

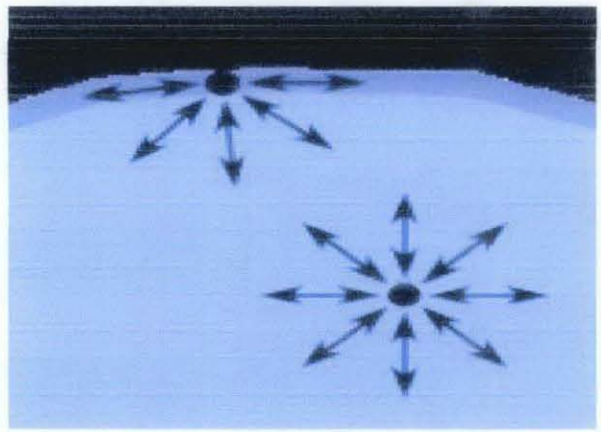

Figure 7 : Illustration of Interfacial Tension of Different Liquids [14]

Interfacial tension is depends on the cohesive forces that exist between the molecules of each liquid, and also the adhesive forces of the molecules of one liquid for those of the other. The interfacial tension of pure oil/water systems can be modified by adding another organic liquid to the oil phase, resulting a change at the interface and hence changes in the cohesive and adhesive forces [15]. Interfacial tension reduction has long

been recognized as one of the most important factors in enhanced oil recovery [16].

J. L. Salager concluded that both low interfacial tensions and a high degree of solubilization are considered desirable for oil recovery [17]. According to Hilton B. de Aguiar , by using sodium dodecyl sulfate (SDS) as stabilizer,the nanofluids can reduce the interfacial tension from 52 mN/m to 10 mN/m by populating the interface [18].

Dielectric nanofluids will help to reduce the interfacial tension by responsing to the EM waves penetrated.This nanofluids will polarize since the metal oxide nanofluid is a bipolar liquid. This action of polarization will altered the cohesive and adhesive force of oil and brine water.Thus, it will recover more oil in enhanced oil recovery.

2.5 Polarization Mechanisms

The interaction of microwaves with dielectric materials causes a polarization of the substance. Several polarization mechanisms can occur including orientation polarization, atomic polarization, electronic polarization, and interfacial polarization as shown in the Figure 8 .

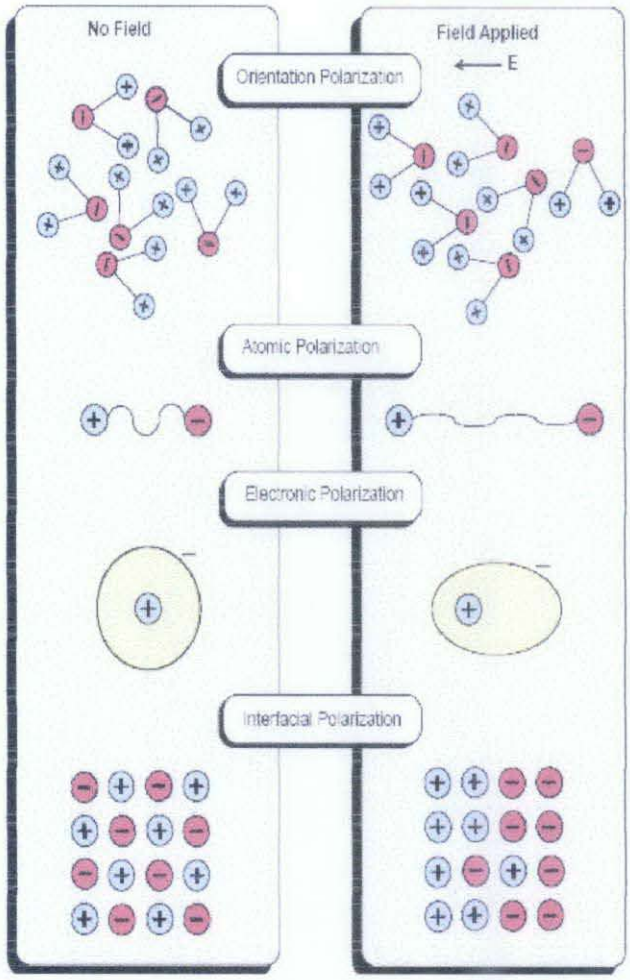

Figure 8 : Schematic representation of the different polarization mechanisms

The various polarization mechanisms all acts differently upon frequency. Thus the relative permittivity, ε^*, will be controlled by different mechanisms as the frequency changes.

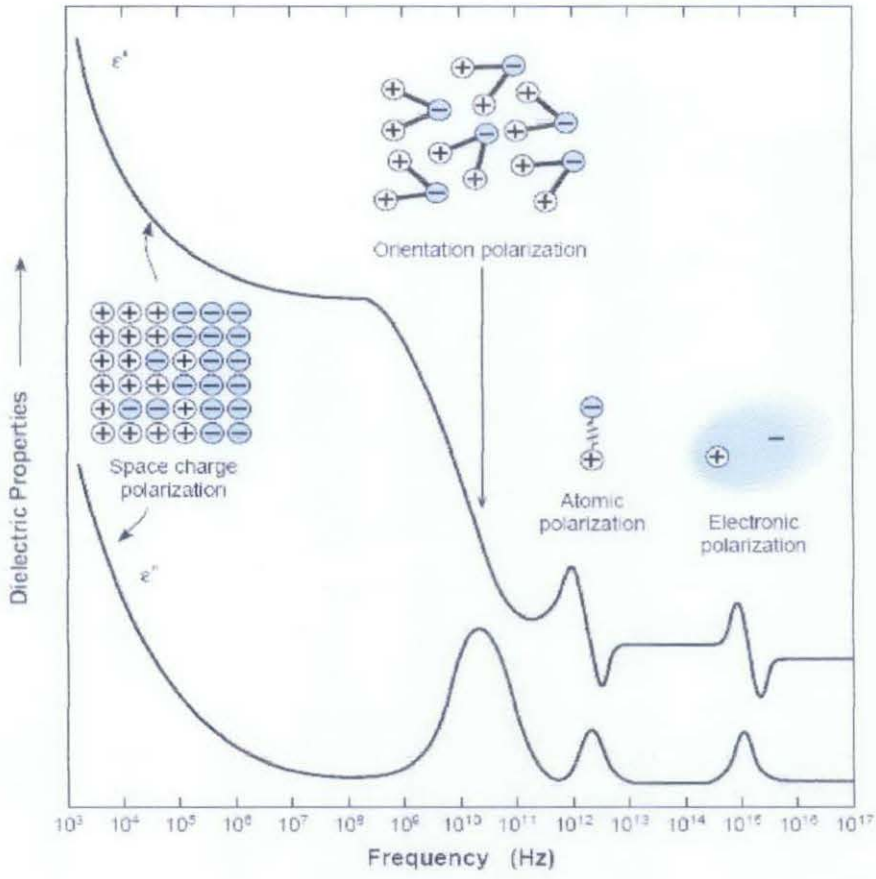

Figure 9 : Contribution of the different polarization mechanisms to the frequency dependence of the relative permittivity

Space charge polarization is also known as interfacial polarization. Throughout this project, we are stressing only on interfacial polarization since the area of interest is to reduce interfacial tension between oil and brine water. Interfacial polarizations exist in any dielectric made up of two or more components having different dielectric constant and conductivities.

In these materials the motion of charge carriers may occur more easily through one phase and therefore are constricted at phase boundaries. As a result, charges build up at interfaces and can be polarized in an applied field. This effect often depends greatly on the conductivities of the phases present.

At low frequency, dielectric properties have its highest peak usually called zero frequency dielectric constant. With increasing the frequency,e* begin to decrease. When the frequency is sufficiently above the relaxation frequency of the polarization that is has no time to form appreciably [19].

CHAPTER 3

METHODOLOGY

3.1 Procedure Identification

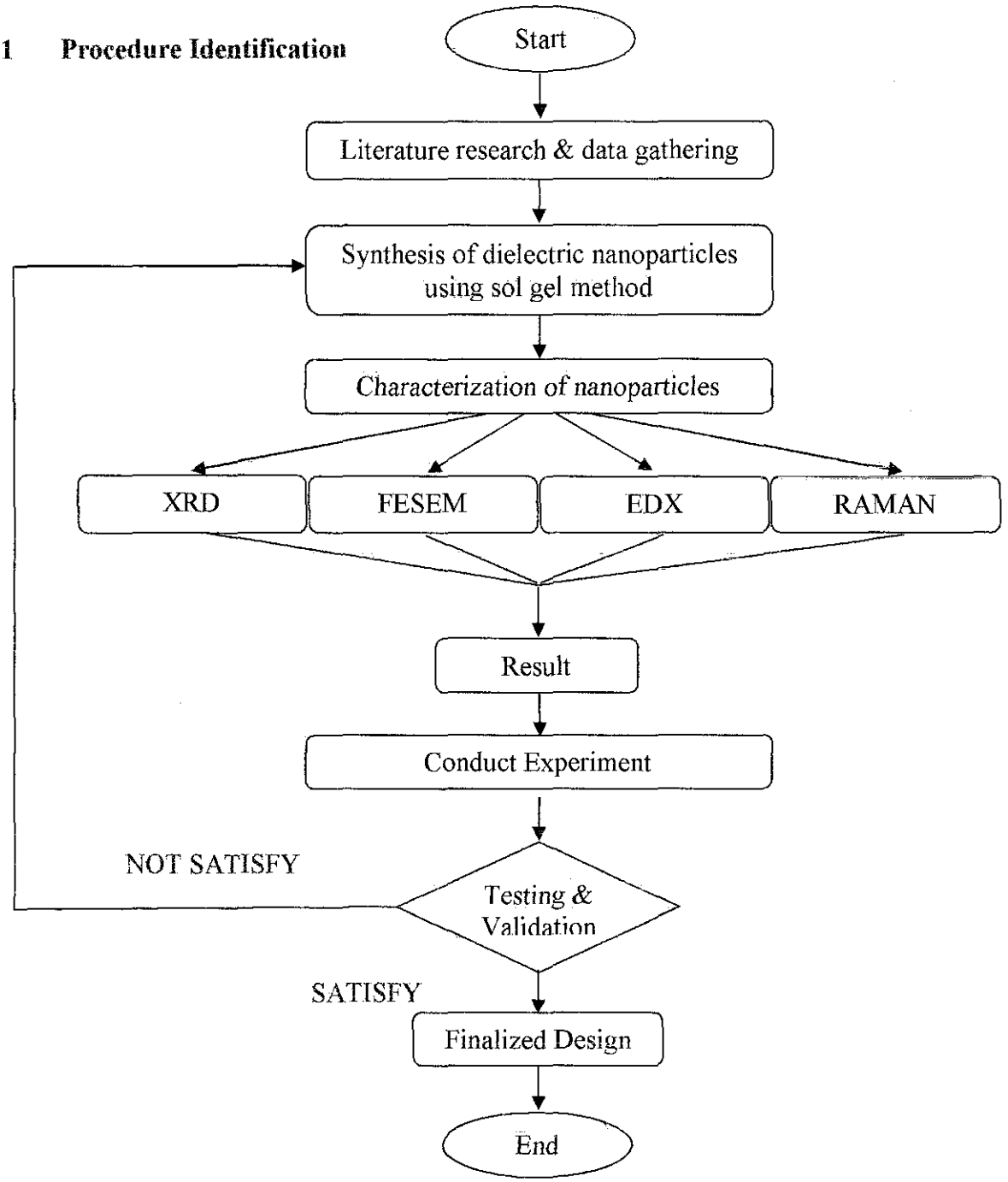

Figure 10: Flowchart of project

3.2 Tools and Equipment Required

3.2.1 Characterization Equipment

- X-Ray Diffraction (XRD)

Diffraction occurs as waves interact with a regular structure whose repeat distance is about the same as the wavelength. It happens that X-rays have wavelengths on the order of a few angstroms, the same as typical interatomic distances in crystalline solids. That means X-rays can be diffracted from minerals which, by definition, are crystalline and have regularly repeating atomic structures.

When certain geometric requirements are met, X-rays scattered from a crystalline solid can constructively interfere, producing a diffracted beam. In 1912, W. L. Bragg recognized a predicatable relationship among several factors.

1. The distance between similar atomic planes in a mineral (the interatomic spacing) which we call the d-spacing and measure in angstroms.
2. The angle of diffraction which we call the theta angle and measure in degrees. For practical reasons the diffractometer measures an angle twice that of the theta angle. Not surprisingly, we call the measured angle '2-theta'.
3. The wavelength of the incident X-radiation, symbolized by the Greek letter lambda and, in our case, equal to 1.54 angstroms [20].

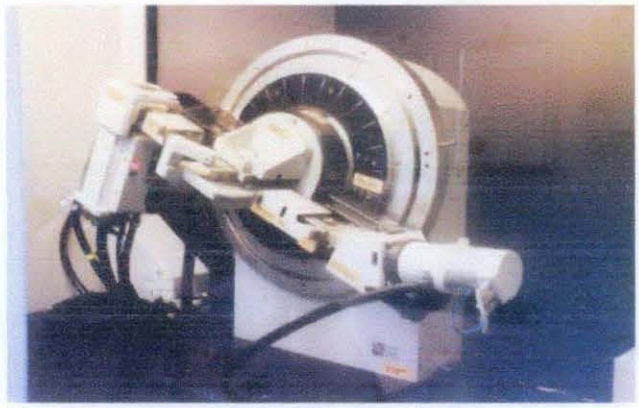

Figure 11 : The Diffractometer

- Field Emission Scanning Electron Microscope (FESEM)

A FESEM is used to visualize very small, may be as small as 1 nanometer topographic details on the surface or entire or fractioned objects. Electrons are liberated from a field emission source and accelerated in a high electrical field gradient. Within the high vacuum column these so-called primary electrons are focussed and deflected by electronic lenses to produce a narrow scan beam that bombards the object.

As a result secondary electrons are emitted from each spot on the object. The angle and velocity of these secondary electrons relates to the surface structure of the object. A detector catches the secondary electrons and produces an electronic signal. This signal is amplified and transformed to a video scan-image that can be seen on a monitor or to a digital image that can be saved and processed further.

Figure 12 : FESEM Equipment

- Energy Dispersive X-ray spectroscopy (EDX)

Energy dispersive X-ray spectroscopy (EDS or EDX) is an analytical technique used for the elemental analysis or chemical characterization of a sample. An electron beam strikes the surface of a conducting sample. The energy of the beam is typically in the range 10-20keV. This causes X-rays to be emitted from the point the material. The energy of the X-rays emitted depends on the material under examination.

The X-rays are generated in a region about 2 microns in depth, and thus EDX is not a surface science technique. By moving the electron beam across the material an image of each element in the sample can be acquired. Due to the low X-ray intensity, images usually take a number of hours to acquire [21].

- RAMAN Spectroscopy

RAMAN Spectroscopy is an analytical technique used to analyze the frequency for samples start to vibrate. Raman scattering may also be interpreted as a shift in vibrational energy state due to the interaction of an incident photon.The incident EM wave induces an oscillating dipole moment, as discussed above, thereby putting the molecular system into a virtual energy state [22].The machine use in Nano Technology Research Laboratory is HORIBAJOBIN VYON.

- LCR vector network analyzer

Agilent LCR vector network analyzer with 16452A test fixture was used to get the data for the initial permittivity, D-factor and Loss Factor for the respective nanofluids.

Figure 13 : LCR vector network analyzer

Figure 14 : 16452A Test Fixture

3.2.2 Hardware

- Transmitter

Transmitter is used to transmit the electromagnetic waves.

- Decaport data acquisition system (DAS) Model NI PXI-1042 and Fluxgate Magnetometer

Fluxgate Magnetometer was used in order to detect EM waves and DAS is used to store the data of the transmitted EM waves.

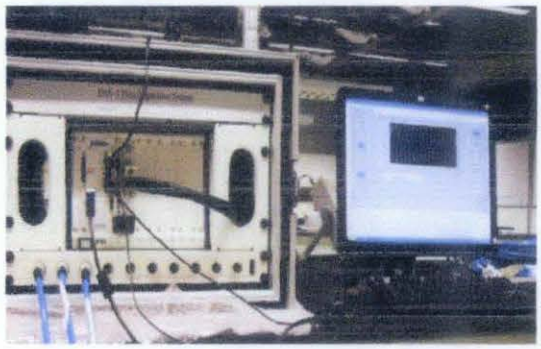

Figure 15: Data Acquisition System

Figure 16: Fluxgate Magnetometer

- Function Generator

INSTEK GFG-8250A f unction generator was used to supply 1 KHz frequency.

Figure 17: Function Generator

- DC Power Supply

ATTEN Electronic DC power supply was used to supply the amplifier with 12V.

Figure 18: DC Power Supply

- Balance

AND GF 3000 balance was used to weigh the materials and core sample. It gives accurate reading up to 4 decimal points.

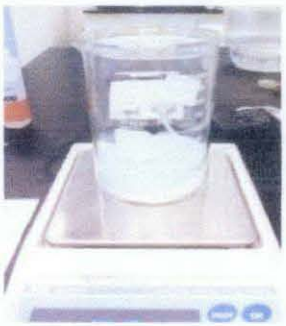

Figure 19 : Balance Machine

- Pressure gauge

Pressure gauge is used to record the pressure value during permeability and porosity test.

Figure 20 : Pressure Gauge

- CAP 2000+ Viscometer

Viscometer was used to measure the viscosity of water, brine and oil.This measurement can be done by putting liquid under the spindle and let the spindle rotate as per set before it give the reading of viscosity values.

Figure 21 : Viscometer

Figure 22 : Variety size of spindle

- MASTERFLEX Console Drive Pump

Masterflex console drive pump is used to flow the brine cylindrical PVC column.

Figure 23 : Consol Drive Pump

- Core sample

To acts as oil core in deep water environment.

Figure 24: PVC Column

CHAPTER 4

RESULTS AND DISCUSSIONS

4.1 Synthesis of Metal Oxide

4.1.1 Experimental Procedure

Metal nitrates such as zinc nitrate hexahydrate, cobalt nitrate hexahydrate , aluminium nitrate nonahydrate and nitric acid (HNO_3), were used as raw materials. All metal nitrates used in the fabrication of metal oxide were dissolved in the aqueous solution of nitric acid HNO_3. Following calculations is done in order to prepare 20g of metal oxide by using sol gel technique. Details of the calculations are simplified in Table 2.

4.1.2 Calculation of metal oxide using sol-gel method

Zinc nitrate hexahydrate [(Zinc $(NO_3)_2.6H_2O$)], cobalt nitrate hexahydrate [$(Co(NO_3)_2.6H_2O)$], aluminium nitrate nonahydrate [$(Al(NO_3)_3.9H_2O)$] , raw material used in preparing metal oxide respectively according to below picture.

Figure 25: Raw material used

- Calculation

Relative molecular mass for Zinc Nitrate

I. Zinc nitrate $(NO_3)_2.6H_2O$ (considering H_2O)

= (65.38) + (2 x 14.0067) + (6 x 15.9994) + (12 x 1.0079) + (6 x 15.994)

= 65.38 + 28.0134 + 95.9964 + 12.0948 + 95.964

= 297.4486 g/mol

II. Zinc nitrate $(NO_3)_2$ (without considering H_2O)

= 297.4486 – (12.0948 + 95.964)

= 189.3898 g/mol

Relative molecular mass for Cobalt Nitrate

I. Cobalt nitrate $[(Co(NO_3)_2.6H_2O)]$ (considering H_2O)

= (58.9332) + (2 x 14.0067) + (6 x 15.9994) + (12 x 1.00794) + (6 x 15.9994)

= 58.9332 + 28.0134 + 95.9964 + 12.09528 + 95.9964

= 291.03468 g/mol

II. Cobalt nitrate $(NO_3)_2$ (without considering H_2O)

= 291.03468 – (12.09528 + 95.9964)

= 182.943 g/mol

Relative molecular mass for Aluminium Nitrate

I. Aluminium nitrate $[(Al\ (NO_3)_3.9H_2O)]$ (considering H_2O)

= (26.981538) + (3 x 14.0067) + (9 x 15.9994) + (18 x 1.00794) + (9 x 15.9994)

= 26.981538 + 42.0201+ 143.9946+ 18.14292 + 143.9946

= 375.133758 g/mol

II. Aluminium nitrate , Al $(NO_3)_3$.(considering H_2O)

= 375.133758 – (18.14292 + 143.9946)

= 212.996238 g/mol

- To prepare 20g of metal oxide

20 gram metal oxide

= (weight material with water / weight material without water) x 20 gram

$$ZnO = \frac{297.4486}{189.3898} \times 20g = 31.41g$$

$$CoO = \frac{291.03468}{182.943} \times 20g = 31.82g$$

$$Al2O3 = \frac{375.133758}{212.996238} \times 20g = 35.23g$$

Table 2 : Calculations for metal oxide

Material	With water	Without water	Gram of material needed	HNO_3 needed
ZnO	297.4486 $gmol^{-1}$	189.3898 $gmol^{-1}$	31.41g	157.05 ml
CoO	291.03468 $gmol^{-1}$	182.943$gmol^{-1}$	31.82g	159.10 ml
Al2O3	375.133758 $gmol^{-1}$	212.996238 $gmol^{-1}$	35.23 g	176.15 ml

HNO_3 needed to dissolve the raw material, and for every 1 gram raw material, 5 ml needed.

4.1.3 Sol Gel Method Procedure

All raw materials needed in synthesizing metal oxide are weight into its corresponding final product weight. The raw materials then are mixed with nitrate acid. After that, the solution was stirred at 250 r.p.m for a week to get high homogeneity solution. After one week of stirring, the solution was heated at 80^0C until gel like solution was formed.

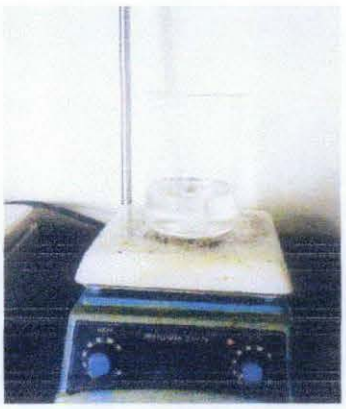

Figure 26 : Stirring process

Figure 27 : Gel formed

Then, the samples were dried in an oven at 110^0C about 3 days for evaporation. After that, the dried samples were crushed for 8 hours to obtain fine particles.

Figure 28 : After drying process

Figure 29 : Crushing process

After that, powers annealed for 6 hours to get required characteristics of metal oxide. Below are the table shows the 2 metal oxide samples with their respective temperatures.

Table 3: Annealing temperature and duration for each sample

Sample	**Temperature (^{0}C)**	**Duration**
ZnO	350	6 hours
	450	
Cobalt oxide	300	6 hours
	400	
Al2O3	1000	6 hours
	1100	

Figure 30: Annealing equipment

Then, the samples were crushed again for 2 hours. Then, these samples were characterized using X-Ray Diffraction (\XRD), Filed Emission Scanning Electron Microscope (FESEM) and Energy Dispersive X-Ray (EDX) and RAMAN Spectrometer.

4.2 Characterization of Nanopowder

4.2.1 X-Ray Diffraction (XRD) Results

The result gathered from the XRD is matched with the standard card of metal oxide nanoparticles. Refer to Table 4.

Table 4: Standard Card of ZnO, CoO and

SAMPLE	STANDARD CARD
ZnO (350°C)	*SS-NNNN 75-0576 (A)*
ZnO(450°C)	*SS-NNNN 75-0576 (A)*
CoO (300°C)	*SS-NNNN 42-1467 (C)*
CoO (400°C)	*SS-NNNN 88-0463 (C)*
Akuminium Oxide (1000°C)	*SS-NNNN 88-1609 (C)*
Akuminium Oxide (1100°C)	*SS-NNNN 81-1667 (C)*

By applying Scherer equation the average crystallite size of the particles can be calculated. The Scherer's equation is: [23]

$$D = \frac{0.9\lambda}{\beta \cos\theta}$$

Where:

K = 0.9 λ = X-ray wavelength (1.5408 Åm)

β = FWHM 2θ θ = Bragg's angle

Values of FWHM 2θ and Bragg's angle are values from XRD analysis.

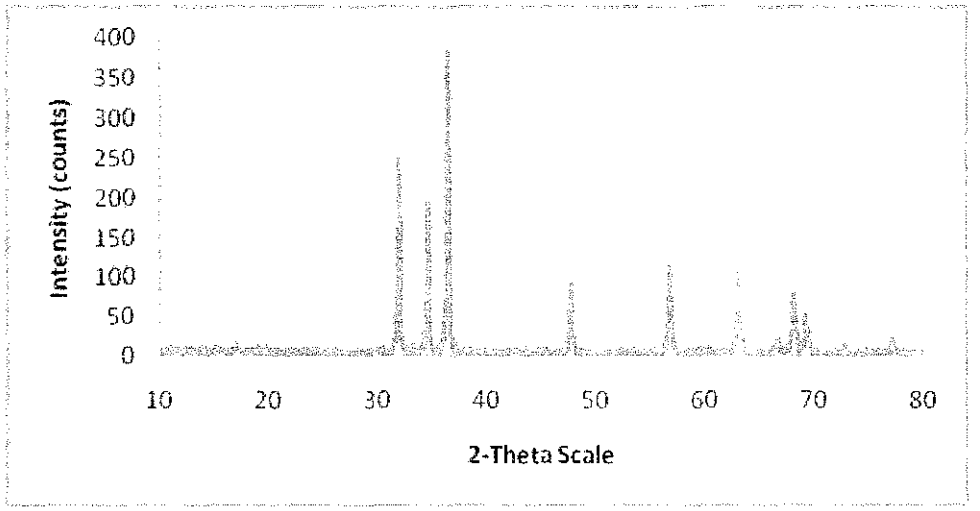

Figure 31: XRD result for ZnO 350°C sample

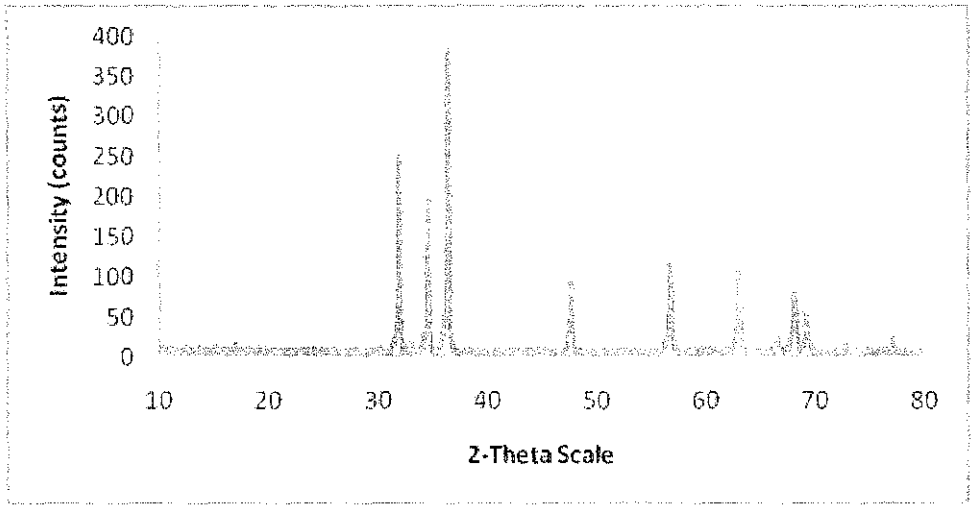

Figure 32: XRD result for ZnO 450°C sample

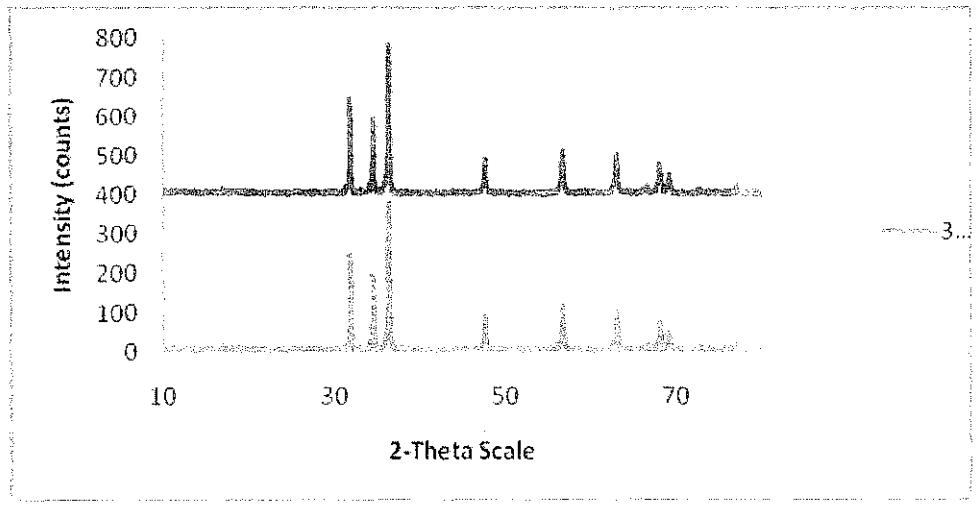

Figure 33: Comparison XRD result for ZnO 350°C and 450°C sample

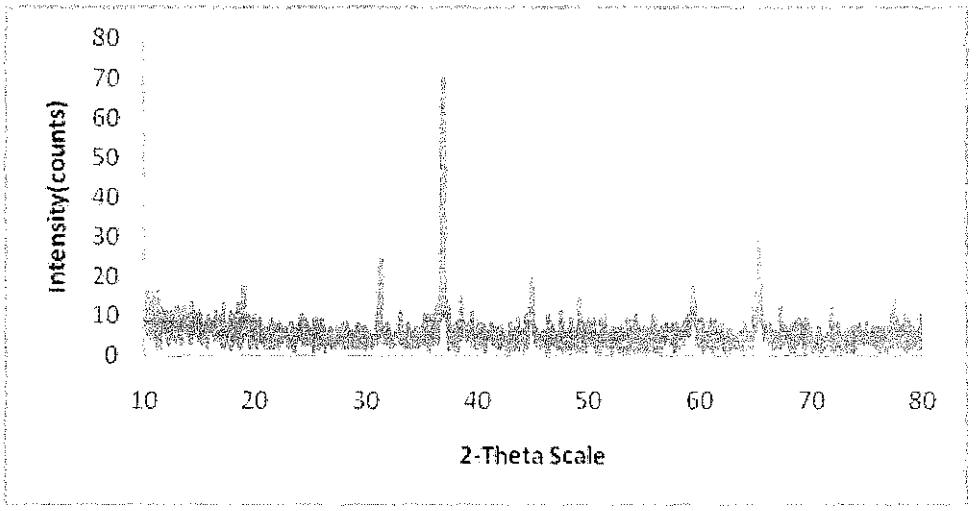

Figure 34: XRD result for CoO 300°C sample

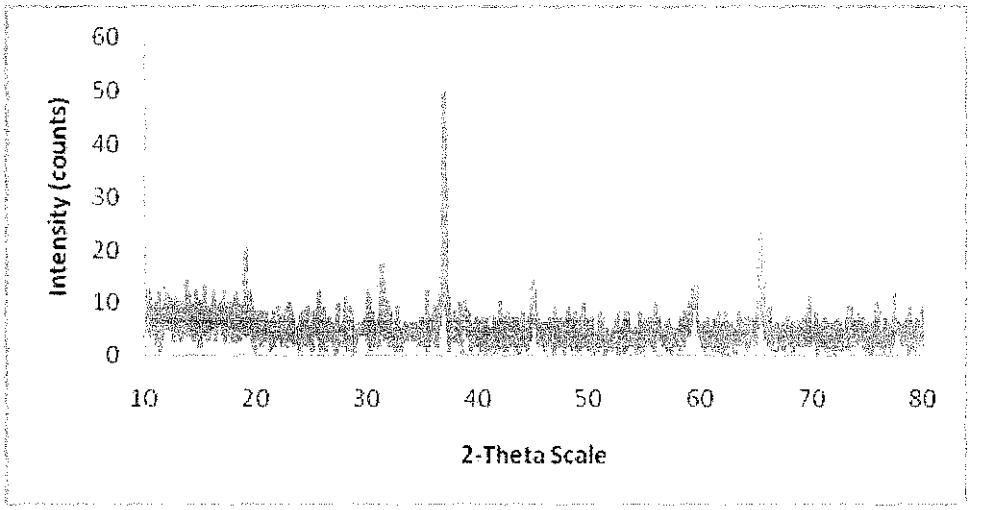

Figure 35: XRD result for CoO 400°C sample

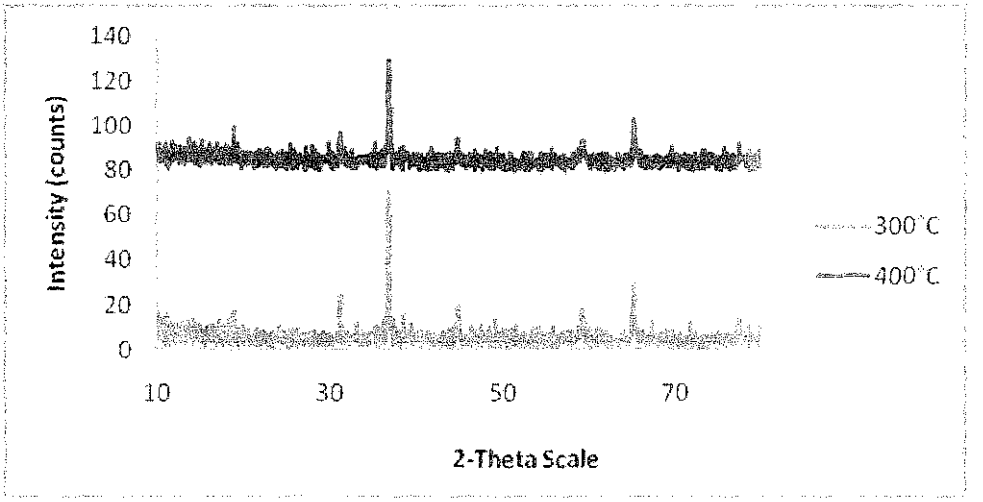

Figure 36: Comparison XRD result for CoO 300°C and 400°C sample

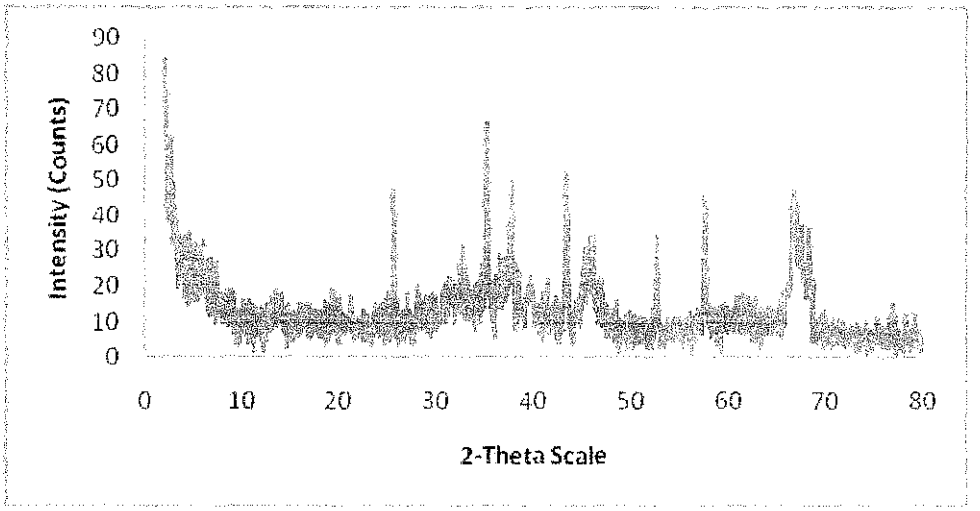

Figure 37 : XRD result for Al_2O_3 1000°C sample

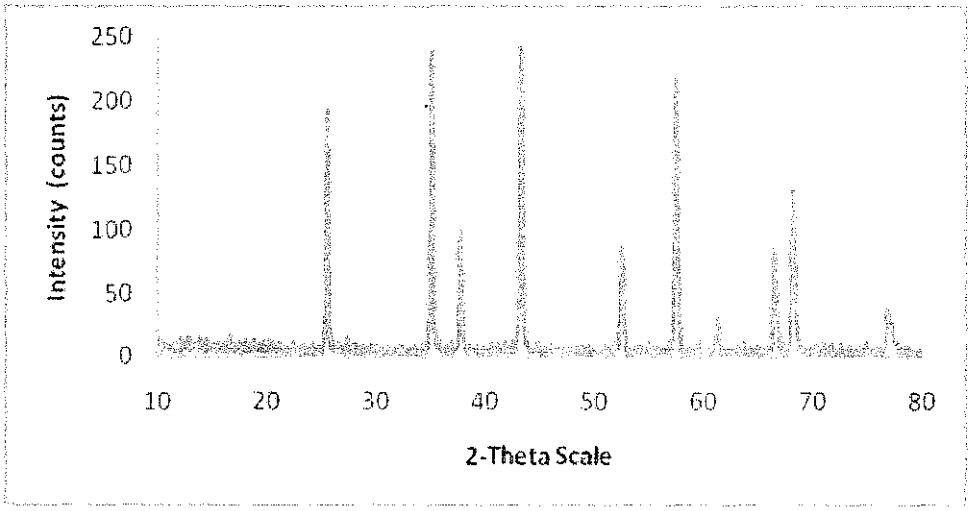

Figure 38: XRD result for Al_2O_3 1100°C sample

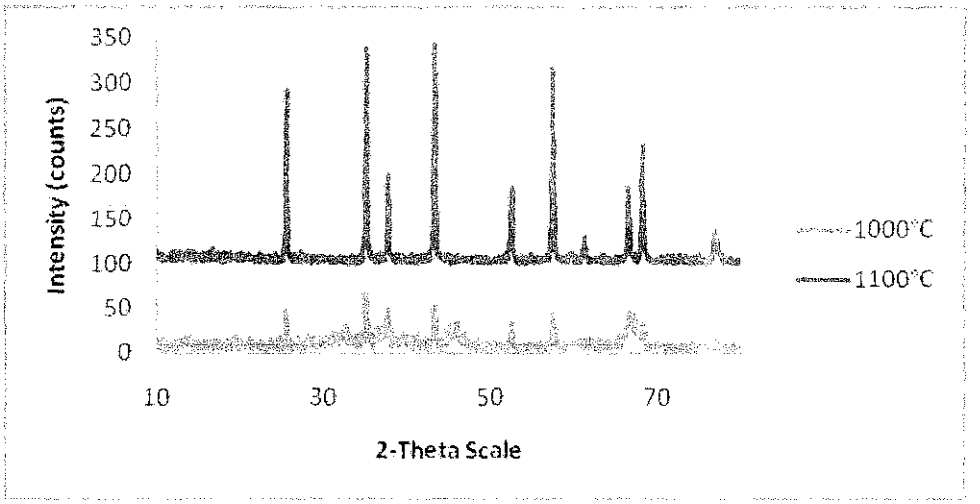

Figure 39: Comparison XRD result for Al_2O_3 1000°C and 1100°C sample

Table 4: XRD data of metal oxide samples with different annealing temperatures

Sample	Temp (°C)	X-Ray Difffraction						
		Intensity (counts)	FWHM	d-spacing	Crystallite size(nm)	a	b	c
ZnO	350	380.95	0.092	2.46241	15.07	3.4982	3.4982	5.20661
	450	380.95	0.113	2.45974	12.27	3.4982	3.4982	5.20661
CoO	300	69.99	0.137	2.43298	10.12	8.0837	8.0837	8.0837
	400	48.99	0.198	2.43028	7.00	8.0837	8.0837	8.0837
Al_2O_3	1000	37.77	0.129	2.38022	93.48	5.5990	5.5990	23.6570
	1100	43.38	0.221	2.084	27.64	4.760	4.760	12.993

Based on the Table 4, XRD analyze the values of full width half maxima (FWHM), d-spacing and crystallite size. To determine the diameter of metal oxide nanoparticle, we used Scherer's equation. For structure, we can claim that ZnO and Al_2O_3 has hexagonal structure because alpha, beta has the same degree while it has different value for gamma. CoO is cubic in size because the alpha, beta and gamma have same degree.

From the table, it is cleared that as we increased the annealing temperature form 350 °C to 450°C of ZnO, from 300°C to 400°C of CoO and from 1000°C to 1100°C the crystallite size decrease and also lattice parameter increases.

Crystallite size obtained from Scherer equation for ZnO are 15.07 nm and 12.27 nm for sample annealed at 350°C and 450°C respectively. Both of the samples have same intensity of 380.95.So, ZnO annealed at 450°C is chosen because of its high intensity and small crystallite size.

For CoO , sample anneal at 300°C is chosen because it have higher intensity than sample anneal at 400°C which is 69.99 even though it has bigger crystallite size of 10.12 nm.

Al_2O_3 annealed at 1100°C chosen because it have higher intensity of 43.38 and smaller crystallite size of 27.64 compared to sample annealed at 1000°C which have low intensity of 37.77 and big size at 93.48 nm.

4.2.2 Field Emission Scanning Electron Microscope (FESEM) Results

Field Emission Scanning Electron Microscope (FESEM) is use to identify the morphology of nanostructure and dimension of grain size for bulk and nanoparticle. Figure 40 and 41 shows FESEM morphology for ZnOannealed at, 350°C and 450°C.

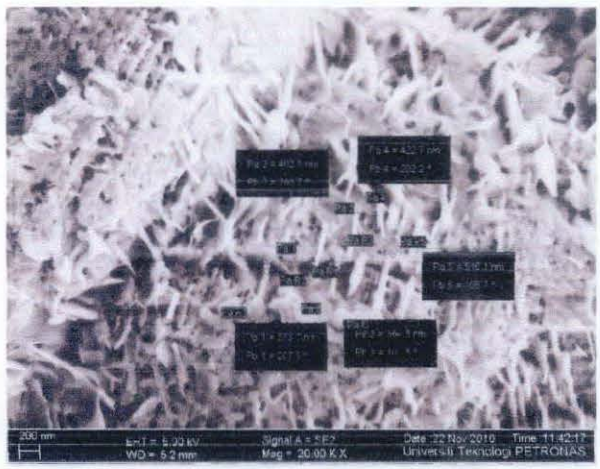

Figure 40: FESEM morphology for ZnO annealed at 350°C

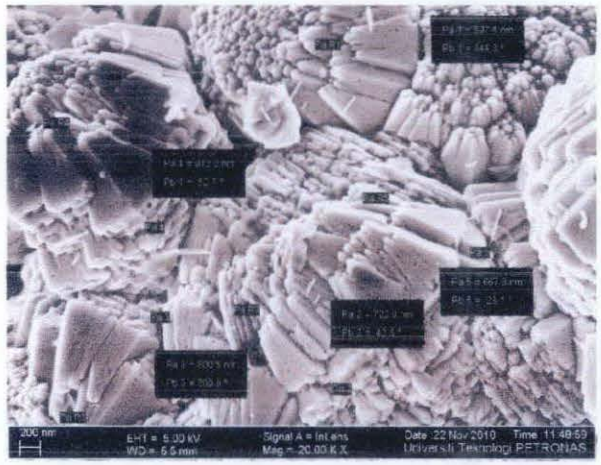

Figure 41: FESEM morphology for ZnO annealed at 450°C

For sample annealed at 350°C, the particle size in the range of 333.7 nm to 516.1 nm. The second sample which annealed at 450 °C, the particle size in the range of 597.4 nm to 912.2 nm. Results show that the grain size is increasing as the sintering temperature increases. Figure 42 and 43 shows FESEM morphology for CoOannealed at 300°C, 400°C.

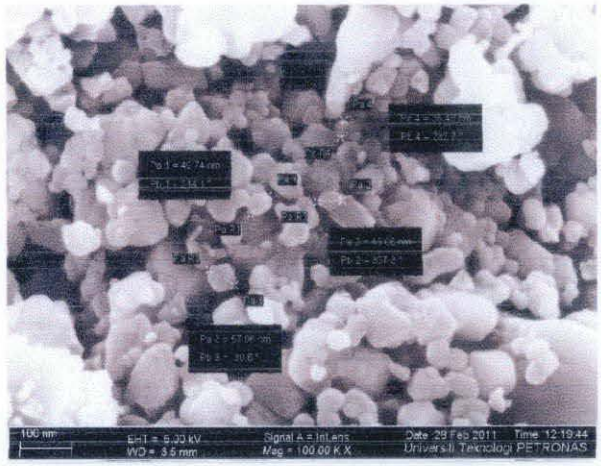

Figure 42: FESEM morphology for CoO annealed at 300°C

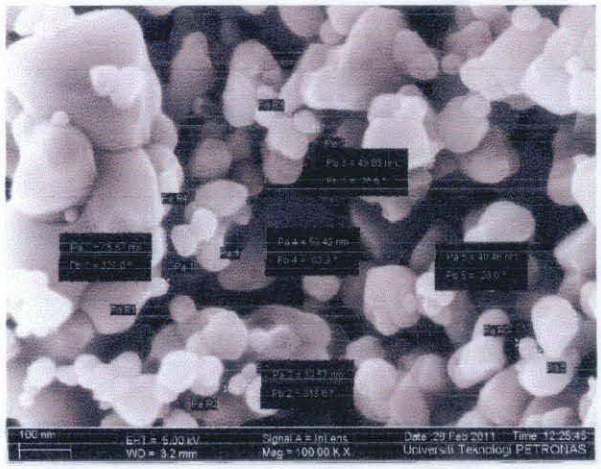

Figure 43: FESEM morphology for CoO annealed at 400°C

For sample annealed at 300°C, the particle size in the range of 35.48 nm to 57.06 nm. The second sample which annealed at 400 °C, the particle size in the range of 39.57 nm to 58.42 nm. Again, increasing sintering temperature resulted increase in grain size.

For sample which annealed at 400 °C for 4 hours, the morphology of CoO became more crystallite for nanoparticles because annealing temperature causes more ions to move into the lattice crystal to be arranged as cubic arrangement.

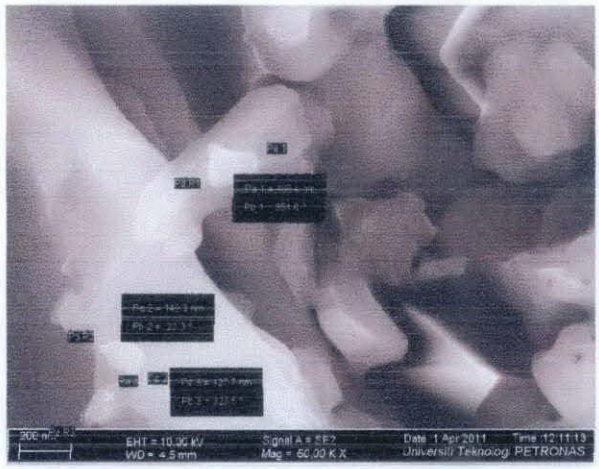

Figure 44: FESEM morphology for Al_2O_3 annealed at 1000°C

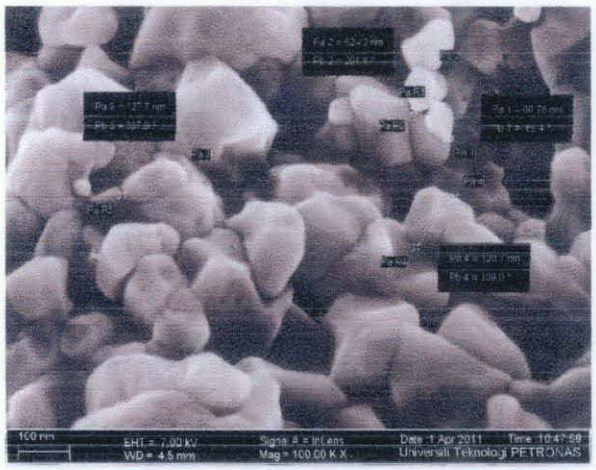

Figure 45: FESEM morphology for Al_2O_3 annealed at 1100°C

For sample annealed at 1000°C, Al_2O_3 particle size in the range of 127.7 nm to 188.4 nm. The second sample which annealed at 1100 °C, the particle size in the range of 66.78 nm to 127.7 nm.

4.2.3 Energy Dispersive X-Ray (EDX)

Energy Dispersive X-Ray (EDX) is a chemical microanalysis technique performed in conjunction with FESEM. Tables below shows that the atomic and weight percentage of the corresponding elements which are Zinc, Cobalt and Oxygen.

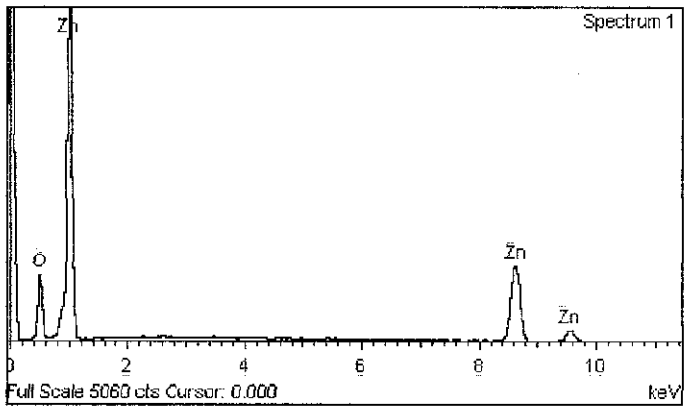

Element	Weight%	Atomic%
O K	23.45	55.59
Zn K	76.55	44.41
Totals	100.00	

Figure 46: Spectrum and EDX data for ZnO 350°C sample

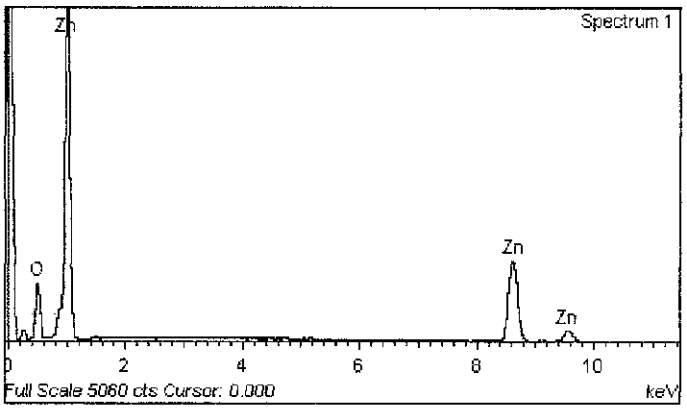

Element	Weight%	Atomic%
O K	20.66	51.54
Zn K	79.34	48.46
Totals	100.00	

Figure 47: Spectrum and EDX data for ZnO 450°C sample

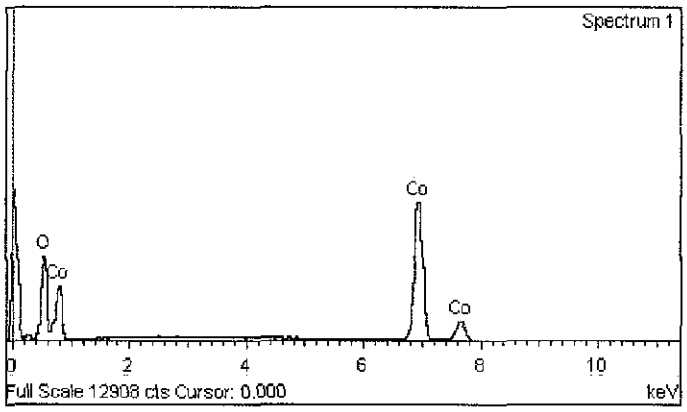

Element	Weight%	Atomic%
O K	24.21	54.05
Co K	75.79	45.95
Totals	100.00	

Figure 48: Spectrum and EDX data for CoO 300°C sample

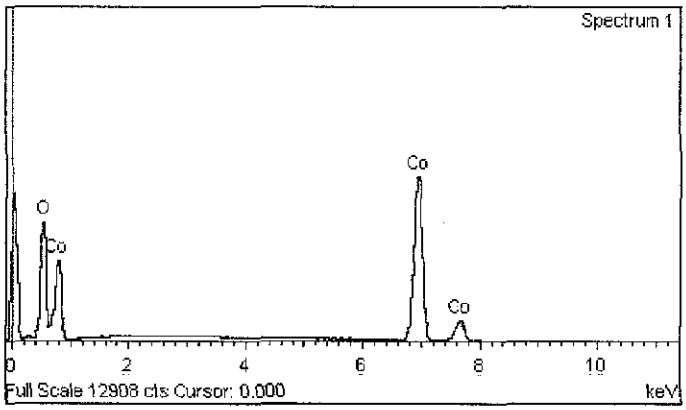

Element	Weight%	Atomic%
O K	27.78	58.63
Co K	72.22	41.37
Totals	100.00	

Figure 49: Spectrum and EDX data for CoO 400°C sample

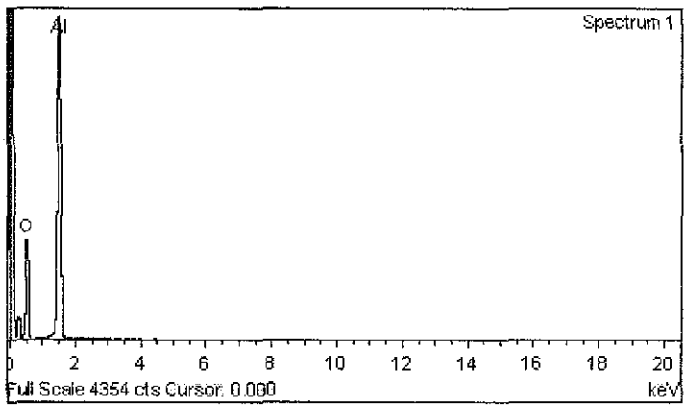

Element	Weight%	Atomic%
O K	52.21	64.82
Al K	47.79	35.18
Totals	100.00	

Figure 50: Spectrum and EDX data for Al_2O_3 1000°C sample

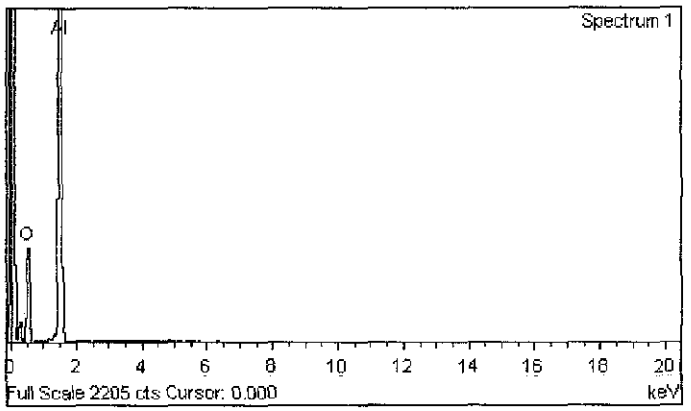

Element	Weight%	Atomic%
O K	50.93	63.64
Al K	49.07	36.36
Totals	100.00	

Figure 51: Spectrum and EDX data for Al_2O_3 1100°C sample

Theoretical values of atomic in percent (%) for metal oxide nanoparticles are calculated as below.

Table 6: Atomic Percentage of Element

Sample		**Elements**	**Atomic Percentage (%)**
ZnO	2	Zinc	½ x 100% = 50%
		Oxygen	½ x 100% = 50%
CoO	2	Cobalt	½ x 100% = 50%
		Oxygen	½ x 100% = 50%
Al_2O_3	5	Aluminium	2/5 x 100% = 40%
		Oxygen	3/5 x 100% = 60%

Table 7: EDX data and standard deviation for ZnO at 350°C and 450°C.

Temperature / Parameter	350°C		450°C	
	Zinc	Oxygen	Zinc	Oxygen
Weight (%)	76.55	23.45	79.34	20.66
Standard deviation (%)	17.00	46.57	21.30	29.13
Atomic (%)	44.41	55.59	48.46	51.54
Standard deviation (%)	11.18	11.18	3.08	3.08

Table 8: EDX data and standard deviation for CoO at 300°C and 400°C.

Temperature / Parameter	300°C		400°C	
	Cobalt	Oxygen	Cobalt	Oxygen
Weight (%)	75.79	24.21	72.22	27.78
Standard deviation (%)	28.6	51.3	22.55	73.63
Atomic (%)	45.95	54.05	41.37	58.63
Standard deviation (%)	8.1	8.1	17.26	17.26

Table 9: EDX data and standard deviation for Al_2O_3 at 1000°C and 1100°C.

Temperature / Parameter	1000°C		1100°C	
	Aluminium	Oxygen	Aluminium	Oxygen
Weight (%)	47.79	52.21	49.07	50.93
Standard deviation (%)	19.48	12.98	22.68	15.12
Atomic (%)	35.18	64.82	36.36	63.64
Standard deviation (%)	12.05	8.03	9.1	6.07

Experimental atomic value is compared with the theoretical atomic value. For ZnO, sample annealed at 450°C is chosen because it has lower atomic deviation of zinc and oxygen at 3.08%.While for CoO, sample anneal at 300°C is better than 400°C because it has atomic deviation of cobalt and oxygen only of 8.1%. Al_2O_3 annealed at 1100°C has atomic deviation of aluminium at 9.1 % and 6.07% of oxygen have deviated. This percent is lower than sample annealed at 1000°C .As conclusion, ZnO ,CoO and Al_2O_3 annealed at 450°C, 300°C and 1100°C respectively chosen to used throughout this project.

4.2.3 RAMAN Spectroscopy Results

Raman shift is expressed in cm^{-1} rather than in Hertz (Hz) because it is more manageable. Since the 1000 cm^{-1} = 299792458 Hz [24].We has the frequency response to the respective samples are as below:

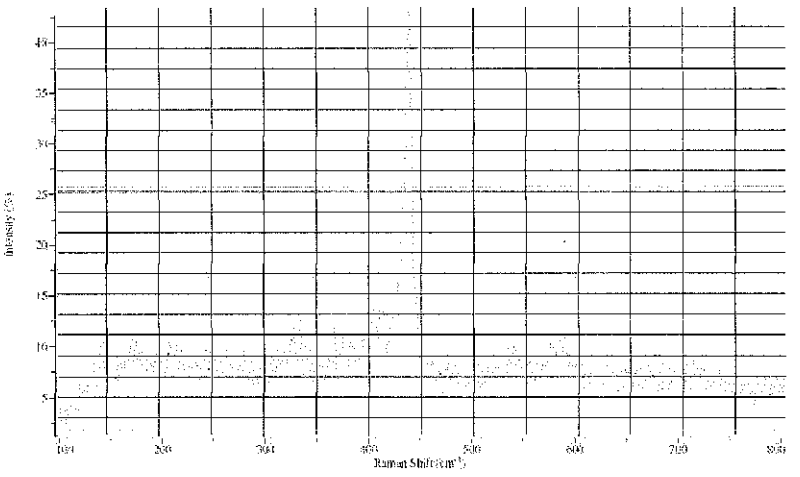

Figure 52: Spectrum RAMAN data for ZnO 350°C sample

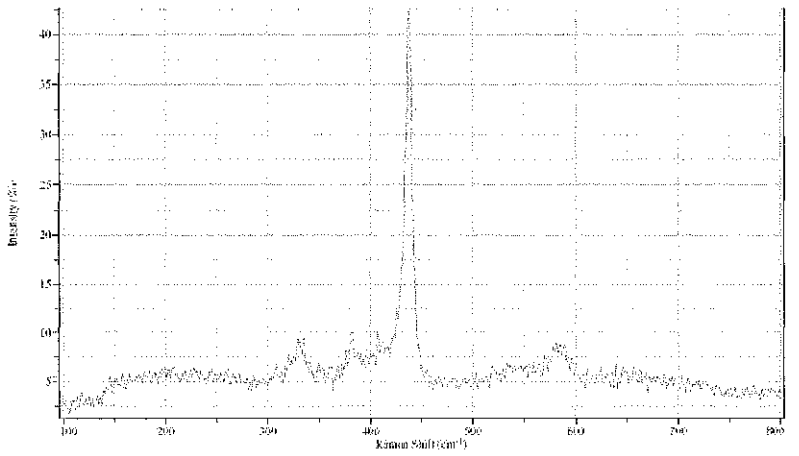

Figure 53: Spectrum RAMAN data for ZnO 450°C sample

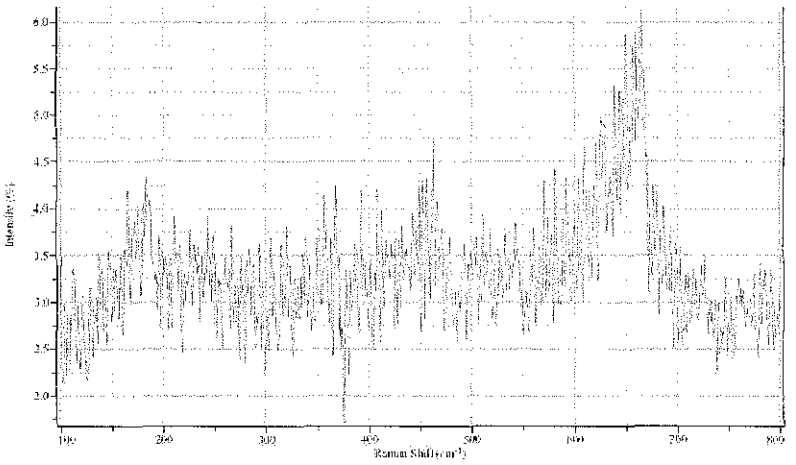

Figure 54: Spectrum RAMAN data for CoO 300°C sample

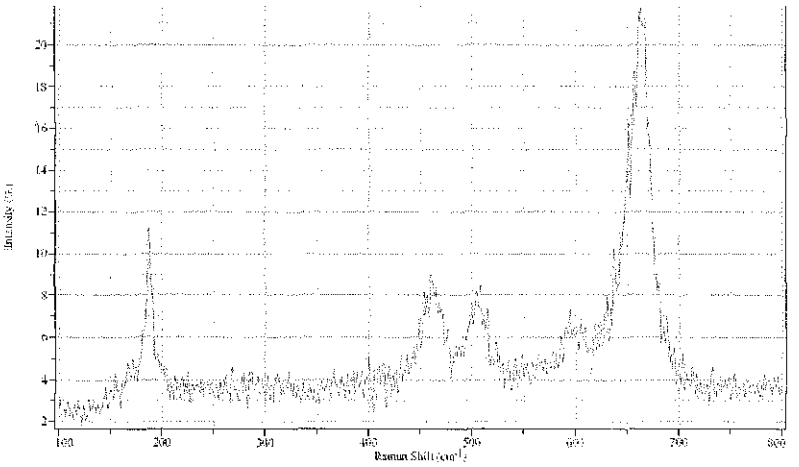

Figure 55: Spectrum RAMAN data for CoO 400°C sample

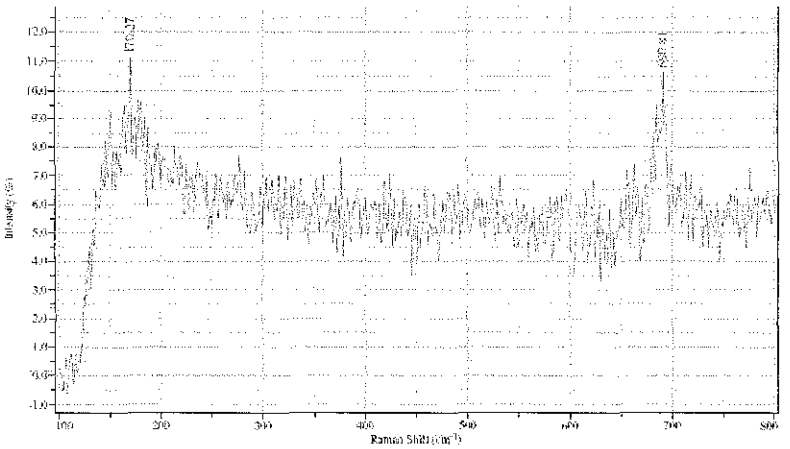

Figure 56: Spectrum RAMAN data for Al_2O_3 1000°C sample

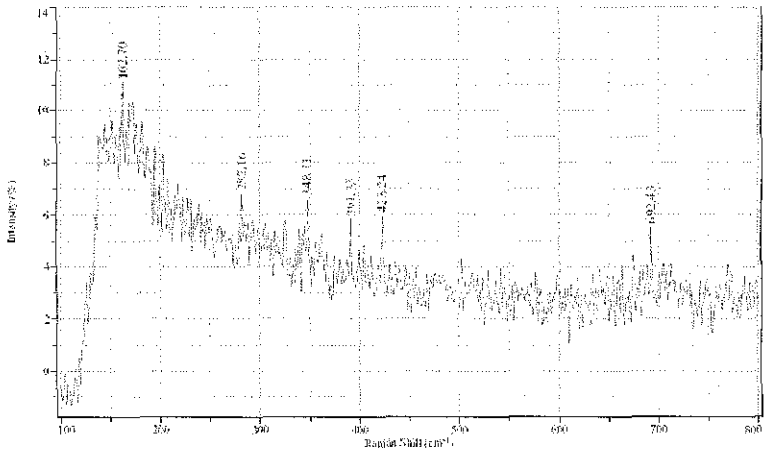

Figure 57 : Spectrum RAMAN data for Al_2O_3 1100°C sample

Table 10 : Nanopowder intensity with respect to its RAMAN shift

Samples	**Highest Intensity (%)**	**Raman Shift (cm^{-1})**	**Hertz (Tera hertz)**
ZnO (350°C)	21.7891	438.378	13.14
ZnO (450°C)	42.2701	437.838	13.13
CoO (300°C)	6.12658	665.405	19.95
CoO (400°C)	21.6708	663.243	19.88
Al_2O_3 (1000°C)	10.4186	170.27	5.105
Al_2O_3 (1100°C)	10.374	162.70	4.88

According to HORIBAJOBIN YVON Application notes, metal oxide are under υ(Xmetal-O) functional group. The letter X is often used to describe variable components; in this case X(metal) means that the variable component is a metallic element. Each group has it own region to indicate whether the vibration is strong or not.

The strong region for metal oxide are ranging from 150 cm^{-1} - 450 cm^{-1} [25].Thus, from the Table 9, we can conclude that ZnO and Al_2O_3 are within the

range but CoO is out of the range. The intensity of the Raman shift of the metal oxide samples decreases when the annealing temperature was increased.

Based on the overall characterization result, ZnO annealed at 450°C,CoO annealed at 300°C and Al_2O_3 annealed at 1100°C chosen to use throughout this project.All these sample have small crystallite size than will affect the reactivity to recover oil.They also have low atomic deviation that nearly resembled to the original percent atom in the sample.

4.3 Petrophysical Characterization

4.3.1 Beads Mixture

Glass beads are used in order to artificially imitate core rock available in reservoirs. In order to find suitable range of porosity, the process began with mixing 3 types of glass beads depends on their size which are ranging from (30-60)μm , (90-100) μm and (425-600) μm. Below are the combination of these three size :

Table 11: Glass Beads Combination

Sample	Combination (180 g)
A	(30-60)μm and (90-100) μm
B	(90-100)μm and (425-600) μm
C	(30-60)μm and (425-600) μm

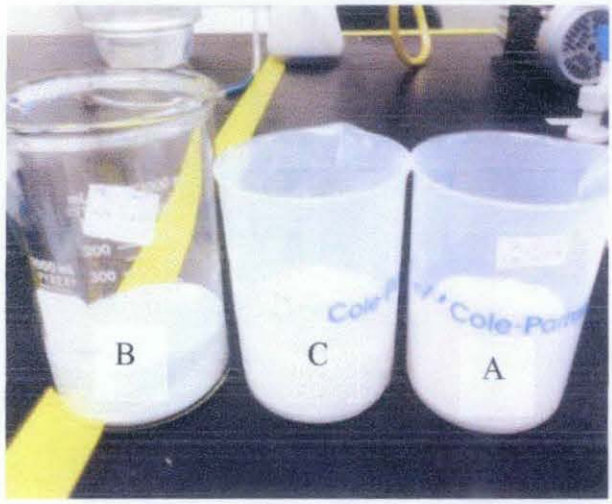

Figure 58: Glass Beads Mixture

Then, the glass beads samples will be filled into the cylindrical PVC column. The weight of cylindrical PVC column with glass beads is recorded for each sample A, B and C.

4.3.2 Permeability Test

Permeability has been commonly symbolized as κ, or k. Permeability is the measure of an ability of the material more commonly of rock or unconsolidated material, to transmit fluids. The measurement of permeability needs to be measured by using Darcy's Law and the unit for permeability is 'Darcy'. The other units are cm^2 and the SI m^2 [26].

According to Darcy Law:

$$k = \frac{q\mu L}{A\Delta p}$$

Where;

k = the permeability of the sample (mD)

q = the flow rate (ml/s)

μ = the viscosity of the fluid (cp)

L = the length of the cylindrical PVC column (cm)

A = the area of the cylindrical PVC column (cm^2)

ΔP = Pressure (atm)

Next, the cylindrical PVC column was set up as shown in Figure 45, where a JASCO PU-2080 Plus pump is used to flow the brine constant flow rate, 2ml/min. Then, the pressure is measured for every 10 minutes for 4 hours or until reach the constant pressure.

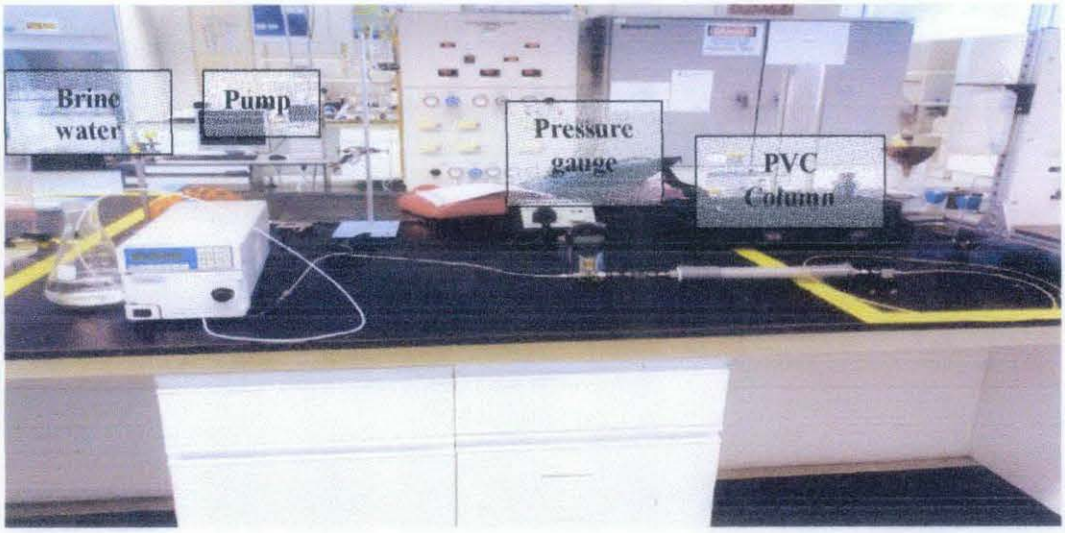

Figure 59: Experiment Set Up for Permeability Test

Table 12: Measurement of Permeability Test

Sample	A	B	C
Flow rate, Q (ml/s)	0.0333	0.0333	0.0333
Viscosity of brine, μ (cp) (at room temperature)	1.02	1.02	1.02
Length of PVC column, L(cm)	22	22	22
Area of PVC column, A (cm^2)	7.0686	7.0686	7.0686
Pressure, ΔP (atm)	0.1973	0.0204	0.0272
Permeability, k (mD)	535.81	5182.07	3886.55

4.3.3 Porosity Test

The porosity is the ratio between the volumes of the pores and that of the rock. When dealing with saturated layers (under the water level, that is to say under the vadose zone where the pores are filled with air and with water), the water content is equal to the porosity [27].

Porosity = (volume of pores) / (volume of the rock)

Volume of the rock can be calculated the volume of the PVC column by calculating cross sectional time the height of the column.

Table 13: Measurement of Porosity Test

Sample	**A**	**B**	**C**
Dry weight (PVC + glass beads) (g)	487.98	496.03	516.06
Wet weight (PVC + glass beads + brine) (g)	536.74	552.52	566.87
Pore mass @ brine mass (wet weight – dry weight) (g)	43.76	56.49	50.81
Brine density (20kppm at room temperature) (g/cm^3)	1.0106	1.0106	1.0106
Pore volume, V_{pore} (Brine mass/brine density) (cm^3)	43.30	55.90	50.28
Bulk volume, V_{pvc} (L x A) (cm^3)	155.5092	155.5092	155.5092
Porosity (%)	27.84	35.95	32.33

Analyzing from both tests, sample A have the have the lowest value compare to the sample B and sample C. This can be concluded that permeability and porosity are dependent to each other. The lower the porosity, the lower permeability.

When the size of the grain is smaller, the smaller the pores are. Then the exposed surface areas are become larger, and this will create larger friction between the flowing fluid and the rock. Thus it will lower the permeability.

Due to low porosity and low permeability ability, sample A is chosen to be core rock sample for this sample. This is because we want to test the ability of the dielectric nanoparticles to recover oil in low porosity and permeability medium.

4.3.4 Stability Test

Nanofluids was mixed with 3 different concentration of stabilizer, 0.1 %,0.5 % and 1 %. Stabilizer used for this test is Sodium Dodecyl Sulphate (SDS).Then, all these samples were put into ultrasonic bath for a 2 hours. After that, these sample are leave for a month and observation had been made every weeks to make sure which of the combination have higher suspension layer.

For the result, 1 % concentration nanofluids with 1% Sodium Dodecyl Sulphate have higher suspension ability and these nanofluids are chosen throughout this project. Higher suspension ability is very important and needed in order for nanofluids suspend longer inside the well in order to recovery more oil.

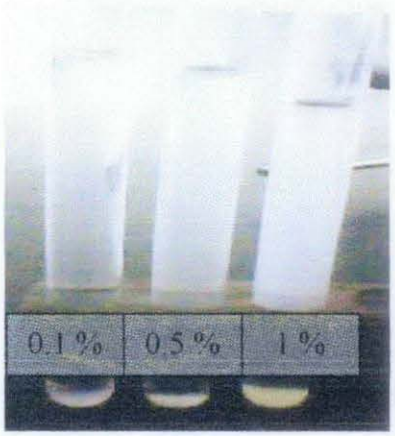

Figure 60: Three concentrations of ZnO nanofluids

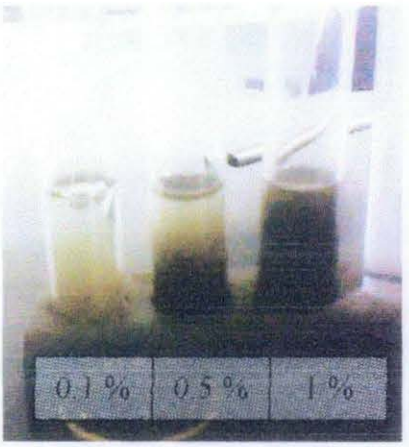

Figure 61: Three concentrations of CoO nanofluids

Figure 62: Three concentrations of Al_2O_3 nanofluids

4.3.5 Dielectric Characterization

The objective of doing the magnetic characterization is to analyse the dielectric constant, relative loss factor (RLF) and dissipation factor (D Factor). LCR vector network analyzer is used to get the data for equivalent parallel capacitance of air, Co and material under, Cp and equivalent parallel resistance of material under test, Rp.

First, nanofluids with 1% concentration with 1% Sodium Dodecyl Sulphate was prepared to perform the dielectric characterization. By using LCR Impedance Analyze together with the 16452A liquid test fixture as shown in Figure 63 below.

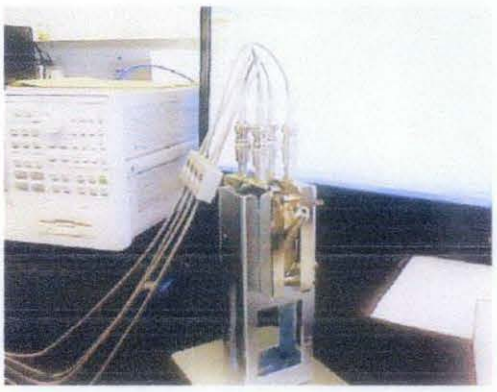

Figure 63 : 16452A Test Fixture

For the first step, 16452A test fixture was assembled and connects to the monitor. After short compensation has been made, air capacitance measured. Then nanofluids poured into the inlet of the fixture. After that Cp-Rp measurement performed with the liquid in the fixture followed by permittivity calculation. Data were recorded. Finally, nanofluids were drain out from the inlet of the fixture.

The formula for dielectric constant, loss factor and dissipation factor are as follow,

Dielectric Constant , $\varepsilon' = Cp / Co$

Relative Loss Factor ,$\varepsilon'' = 1/\omega CoRp$

Dissipation Factor $= \varepsilon''/\varepsilon'$

Where:

Cp = Equivalent parallel capacitance of material under test

Co = Equivalent parallel capacitance of air

Rp = Equivalent parallel resistance of material under test

ω = 2 π f (frequency)

Figure 64,65,and 66 shows the result of the dielectric characterization for ZnO, CoO and Al_2O_3 respectively.

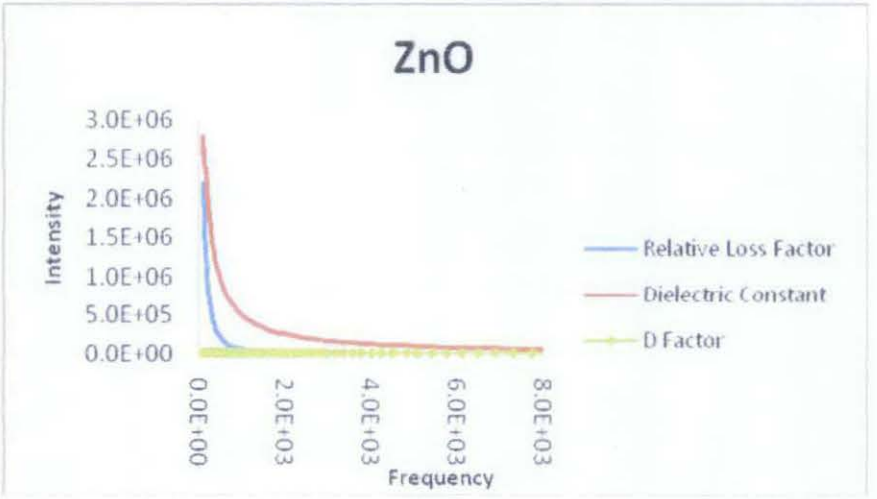

Figure 64: Dielectric characterization for ZnO nanofluid

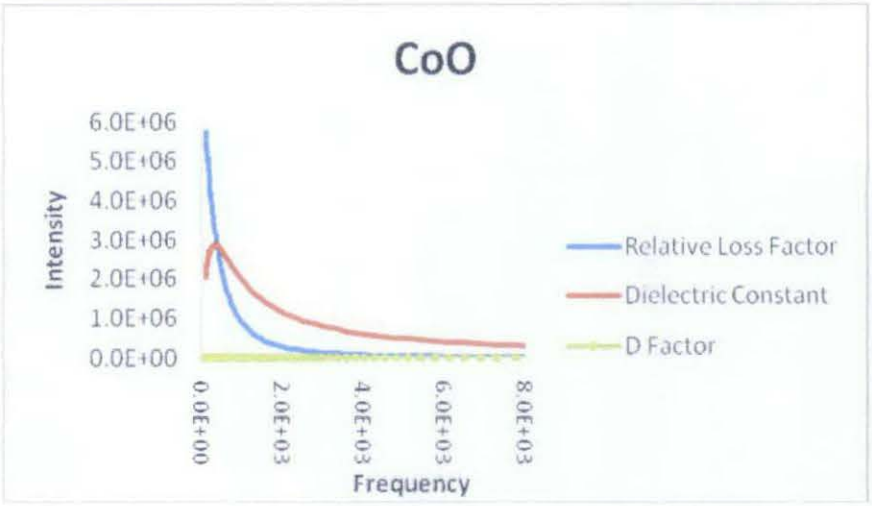

Figure 65: Dielectric characterization for CoO nanofluid

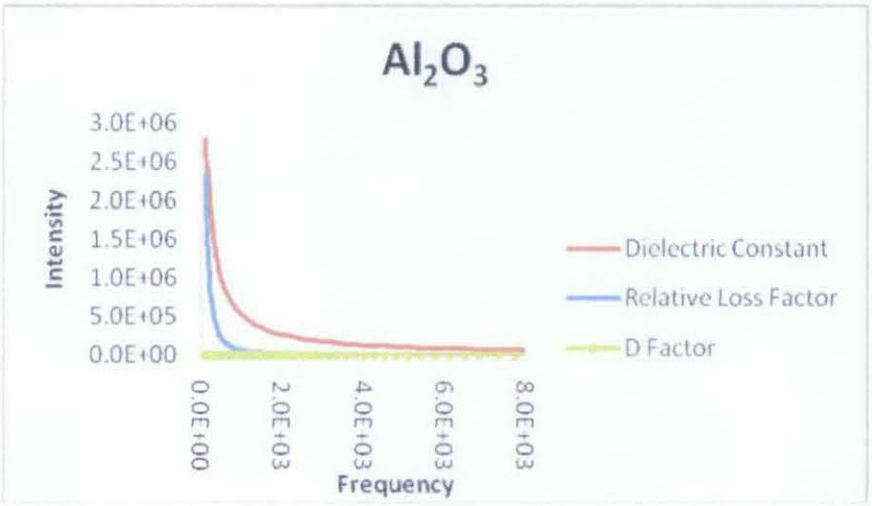

Figure 66: Dielectric characterization for Al_2O_3 nanofluid

Dielectric constant is used to determine the ability of an insulator to store electrical energy. The higher the dielectric constant, the better it is, this is because it can store more of electrical charge. The dielectric constant for all dielectric nanofluids were highest at frequency below 1kHz.Increase in the frequency will reduce the dielectric constant. The interfacial polarization generally occurs at much lower frequencies.

The dielectric constant and relative loss factor (RLF) decreases with increasing frequency. Since the Dissipation Factor (D Factor) is the ratio between Relative Loss Factor and Dielectric Constant, the D factor will constantly in the range of 1 to 10 only.

4.4 Oil Recovery Experiment by using electromagnetic wave transmission.

These experiment aims to evaluate the percentage of oil that can be recover when applying any electromagnetic wave. PVC column first saturated with 20 kppm of brine water until it reach constant pressure.After that,oil was injected into the column. Brine water are collected until no more brine were dispersed out.This volume of brine equal to amount of oil injected into the core.This amount of oil are called Original Oil In Place (OOIP).

Then, we continued with the second brine water injection. This time, brine water will be displacing some of the oil until no more oil coming out from the tube and brine begin to flow. The volumes of oil being displaced from the core sample represent the volume of oil recovered from the secondary recovery (water flooding).Difference between OOIP and Volume of oil recovered from secondary recovery equal to Residual Oil In Place (ROIP).

Experiment continues with nanofluid injection. This time, the transmitter will be activated. The experiment continues until no more oil collected at oil collection section. This volume of oil is the totals of oil that can be recover using nanofluids and transmitter .Figure 66 shows the set up of oil recovery experiment.

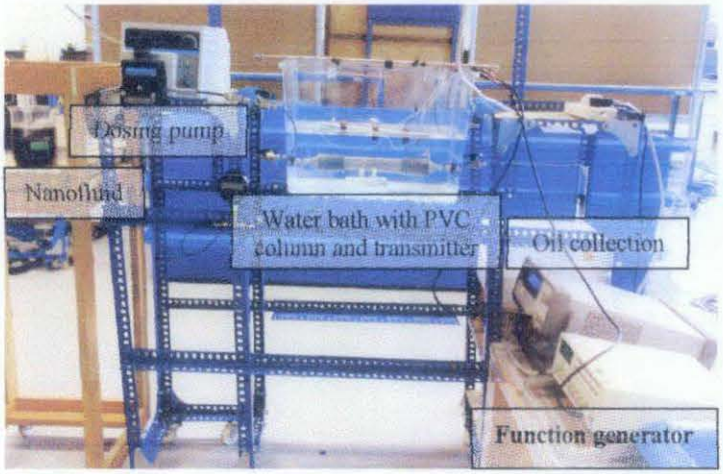

Figure 67 : Experiment Set Up for Oil Recovery Experiment

Steps of the experiment are summarized as below:

A. Using ZnO nanofluids

1. Permeability and pore volume calculated by using Darcy formula and calculation.

Constant parameters:

q = 2ml/min @ 0.333 ml/sec

μ = 1.02 cp

L = 22 cm

A = 7.0686 cm^2

$$\text{Permeability, } k = \frac{Q\mu L}{A\Delta P}$$

Applying Darcy formula, the permeability at pressure of 2.7 psi or 0.1837 is 575.47 mD.

Dry weight = (PVC + glass beads) (g)	487.79
Wet weight = (PVC + glass beads + brine) (g)	542.99
Pore mass @ brine mass = (wet weight – dry weight) (g)	55.2
Brine density (20kppm at room temperature) (g/cm^3)	1.0106
Pore volume, Vv = (Brine mass/brine density) (cm^3)	54.62

2. Original Oil In Place (OOIP) calculation.

After constant pressure is achieved, PVC column was injected with oil until oil drop can be seen at brine collection section. The amount of brine out from PVC column is equal to the amount of oil injected into the column. This represent the amount of OOIP.

OOIP : 52 ml

% OOIP = (Amount of oil displaced / Pore volume) x 100%

= (52 / 54.62) x 100 %

= 95. 2 %

3. Secondary Recovery using water flooding

Brine water was injected for a second time in order to replicate secondary recovery by using water flooding. This step stopped when no more oil drop can be seen out from the outlet. The amount of oil collected represents the oil recovered from this recovery.

Volume of oil collected, $V_{oil, 2nd}$ = 47 ml (assume $1cm^3$ =1ml)

Residual Oil In Place (ROIP) = OOIP - $V_{oil,2nd}$

= 52 ml – 47 ml

= 5 ml

5 ml of oil are left inside the column to be recovered in the 3rd phase recovery or in EOR.

4. Recovery factor for EOR

During this step,nanofluid was injected into the column until there was no more oil drop can be seen at collection section.

Volume of oil collected, $V_{oil, 3rd}$ = 1.55 ml (assume $1cm^3$ =1ml)

% Recovery Factor = ($V_{oil, 3rd}$ / ROIP) x 100%

= (1.55 / 5) x 100 %

= 31 %

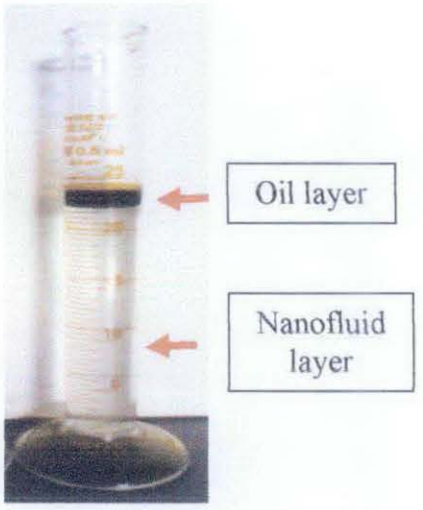

Figure 68 : Oil recovered by using ZnO nanofluid

B. Using CoO nanofluids

5. Permeability and pore volume calculated by using Darcy formula and calculation.

Constant parameters:

q = 2ml/min @ 0.333 ml/sec

μ = 1.02 cp

L = 22 cm

A = 7.0686 cm^2

$$\text{Permeability, } k = \frac{Q\mu L}{A\Delta P}$$

Applying Darcy formula, the permeability at pressure of 2.7 psi or 0.1837 is 575.47 mD.

Dry weight = (PVC + glass beads) (g)	487.79
Wet weight = (PVC + glass beads + brine) (g)	544.28
Pore mass @ brine mass = (wet weight – dry weight) (g)	56.49
Brine density (20kppm at room temperature) (g/cm^3)	1.0106
Pore volume, Vv = (Brine mass/brine density) (cm^3)	55.89

6. Original Oil In Place (OOIP) calculation.

After constant pressure is achieved, PVC column was injected with oil until oil drop can be seen at brine collection section. The amount of brine out from PVC column is equal to the amount of oil injected into the column.This represent the amount of OOIP.

OOIP : 54 ml

% OOIP = (Amount of oil displaced / Pore volume) x 100%

= (54 / 55.89) x 100 %

= 96.62 %

7. Secondary Recovery using water flooding

Brine water was injected for a second time in order to replicate secondary recovery by using water flooding. This step stopped when no more oil drop can be seen out from the outlet. The amount of oil collected represents the oil recovered from this recovery.

Volume of oil collected, $V_{oil, 2nd}$ = 50 ml (assume $1cm^3$ =1ml)

Residual Oil In Place (ROIP) = OOIP - $V_{oil,2nd}$

= 54 ml – 50 ml

= 4 ml

4 ml of oil are left inside the column to be recovered in the 3rd phase recovery or in EOR.

8. Recovery factor for EOR

During this step,nanofluid was injected into the column until there was no more oil drop can be seen at collection section.

Volume of oil collected, $V_{oil, 3rd} = 0.5$ ml (assume $1cm^3 = 1ml$)

% Recovery Factor = ($V_{oil, 3rd}$ / ROIP) x 100%

= (0.5 / 4) x 100 %

= 12.5 %

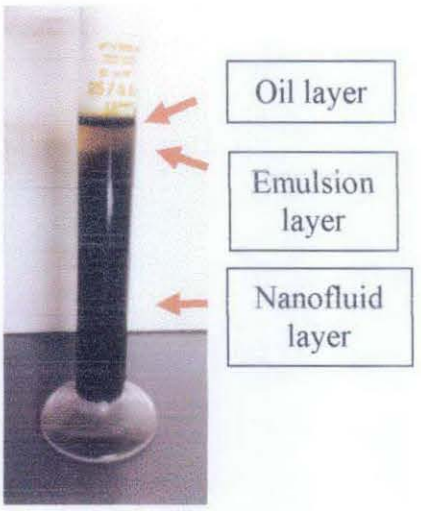

Figure 69 : Oil recovered by using CoO nanofluid

C. Using Al_2O_3 nanofluids

9. Permeability and pore volume calculated by using Darcy formula and calculation.

Constant parameters:

q = 2ml/min @ 0.333 ml/sec

μ = 1.02 cp

L = 22 cm

A = 7.0686 cm^2

$$\text{Permeability, } k = \frac{Q\mu L}{A\Delta P}$$

Applying Darcy formula, the permeability at pressure of 2.7 psi or 0.1837 is 575.47 mD

Dry weight = (PVC + glass beads) (g)	487.79
Wet weight = (PVC + glass beads + brine) (g)	541.35
Pore mass @ brine mass = (wet weight – dry weight) (g)	53.56
Brine density (20kppm at room temperature) (g/cm^3)	1.0106
Pore volume, Vv = (Brine mass/brine density) (cm^3)	52.99

10. Original Oil In Place (OOIP) calculation.

After constant pressure is achieved, PVC column was injected with oil until oil drop can be seen at brine collection section. The amount of brine out from PVC column is equal to the amount of oil injected into the column.This represent the amount of OOIP.

OOIP : 50 ml

% OOIP = (Amount of oil displaced / Pore volume) x 100%

= (50 / 52.99) x 100 %

= 94.36 %

11. Secondary Recovery using water flooding

Brine water was injected for a second time in order to replicate secondary recovery by using water flooding. This step stopped when no more oil drop can be seen out from the outlet. The amount of oil collected represents the oil recovered from this recovery.

Volume of oil collected, $V_{oil,\,2nd}$ = 45 ml (assume $1cm^3$ =1ml)

Residual Oil In Place (ROIP) = OOIP - $V_{oil,2nd}$

= 50 ml – 45 ml

= 5 ml

5 ml of oil are left inside the column to be recovered in the 3rd phase recovery or in EOR.

12. Recovery factor for EOR

During this step,nanofluid was injected into the column until there was no more oil drop can be seen at collection section.

Volume of oil collected, $V_{oil, 3rd} = 0.5$ ml (assume $1cm^3 = 1ml$)

% Recovery Factor = ($V_{oil, 3rd}$ / ROIP) x 100%

= (0.5 / 5) x 100 %

= 10%

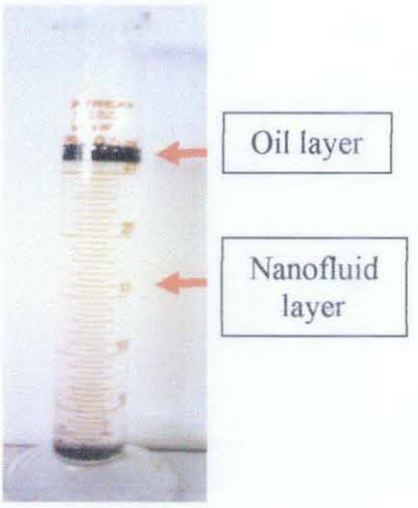

Figure 70 : Oil recovered by using Al_2O_3 nanofluid

From this experiment, ZnO nanofluid successfully recovered about 31 % of oil from OOIP compare to Al_2O_3 and CoO that recovered 20 % and 12.5 % respectively.

CHAPTER 5

CONCLUSION AND RECOMMENDATION

5.1 Conclusion

By using sol gel method, metal oxide of ZnO , CoO and Al_2O_3 was successfully synthesized. All these three metal oxide were prepared at low temperature have good structure, high intensity, small grain size below 30 nm and also have good dielectric properties.

From oil recovery experiment, ZnO yields highest percentage of oil recovery which is 31 % while for CoO and Al_2O_3, they recovered about 12.5 % and 20 % respectively. It is proven that dielectric nanoparticles can be the enhancer to recovery more oil.

The major finding in this project is the stability of the nanofluids. During stability test, 1% nanofluids were mixed with 0.1%, 0.5 % and 1% of Sodium Dodecyl Sulphate (SDS).This SDS act as stabilizer. After 2 hours of ultrasonic bathing,these sample are leave it for a month. Observation had been made for every 1 week.After 1 months, nanofluid mized with 1% of SDS have least precipitate and have most cloudiest mixture compared with nanofluids with 0.1%, 0.5 % of SDS.This showed that this nanofluids have the ability to suspend longer when it injected into the well.

5.2 Recommendation

There are lots parameter can be changes in order to improve the project and get more accurate results. Below are some recommendations:

1. Add another parameter during oil recovery experiment such as temperature and pressure.
2. Ensure that particle size is about the same to make sure all particles can be suspended in water during core flooding.
3. Varies the distance between core rock sample, transmitter and decaport.

REFERENCES

[1] Ainsley Jolley, "The Supply of Fossil Fuels Climate Change", Working Paper No. 9 Climate Change Project Working Paper Series March, 2006.

[2] Willem Schulte, "Shell Chief Scientist Reservoir Engineering, Leading on Innovation ", Summer, 2008.

[3] Uren, L.D. and Fahmy, " Electromagnetic Heating, Transmission", pp. 318—335, 1927.

[4] Zhang Jihong, Yu Haiming, Wang Yanan, Zhang Gang, "Experimental Research On Further Enhanced Oil Recovery By Using High DC Electric Field", November, 2009.

[5] "Nanoparticles" retrieved on 28th August 2010 from http://www.trynano.org/nanoparticles.html

[6] X.W.SUN, C.X.XU, "Growth and Characterization of Misostructural Zinc Oxide Tubes", Journal of Metastable and Nanocrystalline Materials, pp. 23-293, 2005.

[7] J.B.Wua, J.P. Tua, X.L.Wanga,W.K. Zhang, "Synthesis of Nanoscale CoO Particles and Their Effect on The Positive Electrodes of Nickel–Metal Hydride Batteries", 4 August 2006.

[8] I.Luisetto, F.Pepe, E.Bemporad, "Preparation and Characterization of Nano Cobalt Oxide", Supplement 1, Vol.10, pp. 59-67, 1999.

[9] Dr. Martin Kearn, "Development and Applications of Ultrafine Aluminium Powders", 31 December 2003.

[10] S.A Corr, Y.K Gun'ko, A.P Douvalis, M.Venkatesan and R.D. Gunning, "Magnetite Nanosrystal from a Single Source Metallorganic Precursor: Metallorgani Chemistry vs Biogeneric Bacteria", Master Chemistry, Vol.14, pp. 94, 2004.

[11] Tortella E, Morelli M R, Kiminami RHGA, "Mater Sci Forum, Costa ACFM ", pp. 416–418, 2003.

[12] D. Niznansky, J. Luc Rehspringer and M. Drillon, "Preparation of Magnetic Nanoparticles (Y-Fe_2O_3) In The Silica Matrix ", March 1994.

[13] R. Kornak, D. NižňanskÝ, K. Haimann, W.Tylus, K.Maruszewski, "Synthesis of Magnetic Nanoparticles Via The Sol-Gel Technique", 2005.

[14] C. Moules, "The Role of Interfacial Tension Measurement in the Oil Industry", Camtel Ltd, 2009.

[15] "Prediction of Interfacial Tension between Oil Mixtures and Water", Journal of Colloid and Interface Science, pp. 509–513, 2001.

[16] U. Aslam, "Numerical Simulation of Surfactant Flooding in Mixed Wet Reservoirs", pp. 25, 2010.

[17] J. L. Salager, J. C. Morgan, R. S. Schechter, W. H. Wade, E.Vasque, "Optimum Formulation of Surfactant/Water/Oil Systems for Minimum Interfacial Tension or Phase Behavior", 2009.

[18] Hilton B. De Aguiar, Alex G. F. De Beer, Matthew L. Strader, and Sylvie Roke, "The Interfacial Tension of Nanoscopic Oil Droplets in Water Is Hardly Affected by SDS Surfactant", 2010.

[19] J.Murphy and S.O.Morgan, "The Dielectric Properties of Insulating Materials", pp. 493-512, 2008.

[20] "Some Background about X-Ray Diffraction" retrieved on 4th September 2010 from http://www.geosci.ipfw.edu/XRD/techniqueinformation.html

[21] "Energy Dispersive X-Ray Spectroscopy" retrieved on September 2010 from http://en.wikipedia.org/wiki/Energy-dispersive_X-ray_spectroscopy

[22] Derek A. Long, "The Raman Effect", John Wiley & Sons, 2002.

[23] "Derivation of Scherrer Relation Using an Approach in Basic Physics Course", Nanoscience & Nanotechnology Journal Vol. 1(1), Februari 2008.

[24] "Energy Conversion Factors" retrieved on January 2011 from http://optics.unige.ch/convert.htm

[25] "Raman Spectroscopy for Analysis and Monitoring" retrieved on March 2011 from http://www.horiba.com

[26] "Permeability (Fluid)" retrieved on 10th March 2011 from http://www.absoluteastronomy.com/topics/permeability(fluid)

[27] "Short note on the Principles of Geophysical Methods for Groundwater Investigations", retrieved on 15th March 2011 from http://www.geo-hydrology.com